

Effects of Gating System and Casting Geometry on Oxide Inclusions in Steel Castings

Robert Donahue, Richard A. Hardin and Christoph Beckermann

**Solidification Laboratory
Department of Mechanical Engineering
The University of Iowa, Iowa City, 52242**

Abstract

Results from two series of casting experiments are presented investigating two important topics related to producing cleaner steel castings by controlling of oxide inclusions; generation of inclusions in the casting system, and their transport and final locations in the casting system. In the first series of experiment, cases were designed to study effects of gating system on air entrainment, and metal delivery to the mold on casting cleanliness. The objective of the second series of experiments was to generate inclusions, and to study the effects of casting shape and surface orientation on the final inclusion locations and distribution within the casting. Three methods were developed to inspect and measure the inclusions in the experiments using radiography, and surface inspection for inclusions on as-cast and media blasted cope surfaces. Media blasting the cope surfaces prior to inspection was found to be most trustworthy, accurate and best direct inclusion measurement method. In the gating system experiments hardly any inclusions were found to be generated in the gating. This was determined by positioning filters to isolate sources of the inclusions. The primary source of inclusions was from the ladle, and the pouring cup. The inclusions measured in the castings are significantly higher for all cases without using a filter. The dirtiest castings poured used the tallest sprue height (27") with no metal filtering. The tallest sprue height cases with filter in the runner were expected to be among the cleanest, and it was in one of the two heats it was poured. In the other heat it was the third dirtiest casting out all 13 sprue height experiments. The 17" and 22" tall sprue cases with filter at the cup outlet were consistently the cleanest castings. The inclusion tracking experiments showed that inclusions are not evenly distributed in a casting, except on the cope surface of a horizontal plate. It is found that the location and geometry of the gating system and orientation of casting cope surfaces affect the distribution of inclusions in the castings.

Introduction

Oxide inclusions in steel castings are estimated to contribute 20% to the cost of a casting due to the costs of removing them and repairing the casting [1]. They are also a frequent cause of premature failure of steel castings when not detected during production. There are numerous sources of oxides such as the ladle lining and poorly deoxidized melt, and many casting process variables can affect the levels of oxides in steel castings. The cleanliness the melt can vary from heat to heat, so called dirty heat versus clean heat, due to poor control the melt practice. Considering all the sources of oxide inclusions, reoxidation inclusions, formed during pouring of the metal into the mold, are a common cause of inclusion defects in steel castings, if not the most common. Reoxidation inclusions form when deoxidized steel comes into contact with

oxygen during mold filling. They are reported to make up 83% of oxide inclusions in low-alloy steel castings and 48% of inclusions found in high-alloy steel castings [2]. Reoxidation of the steel during pouring can be minimized by employing well designed gating systems. Much research has been performed for over 50 years to establish rules for gating castings. However, the design of gating systems is still more of an art than a science.

This paper presents the results from two series of casting experiments investigating perhaps the two most important topics related to the control of oxide inclusions in steel casting; 1) their generation in the casting system and 2) their transport and final locations. So the reader will find this paper is organized by presenting the clean steel casting experiments and results in two parts.

The objective of the first part of these experiments was to investigate the effect of different gating system design approaches on the formation of reoxidation inclusions. Experiment cases in the first part were designed to study effect of gating system on air entrainment and metal delivery to the mold on casting cleanliness. These experimental cases include: a simple non-pressurized “open” gating system (an assumed poor quality case); a pressurized gating system with pouring basin, good flow control, minimization of air entrainment (an assumed best quality case using best practice gating system design); cases having various sprue/falling heights of metal during filling; and cases using a filter for flow control, cleaner metal, placed at different locations in the gating system to try to isolate and pinpoint locations and sources of inclusion generation. The first section of the paper is the “Gating Study.”

In the second series of experiments presented here, the objective was to generate inclusions and produce flow patterns in various casting geometries to study the effects of casting shape and surface orientation on the final inclusion locations and distribution within the casting. Another objective of obtaining this experimental data is to compare results with an air entrainment model that includes inclusion generation and tracking. Analysis of these comparisons will allow for calibration and validation of the model. Even without their use in model validation, the experimental results will improve our understanding of the effects of various casting geometric features on the final locations of inclusions in castings. The second section of the paper is the “Inclusion Tracking Study.” Before presenting any results, the measurement and analysis procedures are described.

Inclusion Measurement Methods, Analysis Procedures and Other Considerations

The clean steel experiments were quantitatively analyzed and inclusions were measured using three methods. The procedures used in the methods are described below. In the first method, quantitative analysis of radiographs was used to measure the inclusion indications present in the uppermost ½” section of the casting experiments’ cope surfaces. These indications are mostly gases generated by the oxide formation. In the second method the as-cast cope surface of the experiment is inspected and inclusions are marked. In the third method the cope surface is blasted with media, cleaning it to expose inclusion pits, and then inspected and inclusions marked. In both the second and third methods, the marked areas of inclusions are digitized into, and quantitatively analyzed, using image analysis software. Additional procedures and considerations related to the design and analysis of the experiments are also described below. In

all experiments, ASTM A216 WCB steel was poured at the University of Northern Iowa Metal Casting Center.

Inclusion Measurement Method 1: Quantitative X-Ray Analysis

The quantitative analysis process of radiographs of the casting experiments is illustrated by the series of images in Figure 1. For the casting geometry used in the first series experiments to investigate gating systems, a 6" x 6" x 3" block casting (Figure 1 upper left image) is used. The experiments were designed using a chill on the cope surface to produce sound material (shrinkage porosity free) having a sufficient thickness. The majority of the inclusions generated in the experiments are trapped near the cope surface where they can be measured. It was determined that a 0.5" thick section of the cope surface was a sufficient thickness and volume for collecting the majority of the inclusions in the casting. The cope surface was cut off as shown in the upper middle image in Figure 1 to create a cope surface slice as shown upper right image in Figure 1. The bottom surface of the slice was machined to create a uniform nominal thickness (bottom left image in Figure 1).

The cope slice of steel was digitally radiographed. The indications in the radiograph (round darker regions) are, for the most part, gas byproduct voids around inclusions formed in the reaction between the steel and air. The quantitative x-ray analysis procedure used is described in detail elsewhere [3]. It is described here briefly with reference to Figure 1. As shown in the "x-ray layout image" in the figure, a steel stepped block with a series thicknesses was radiographed with each cope slice. Using the gray levels of the steps and their thicknesses, a calibration procedure was performed for each image to determine a gray level thickness curve. From this curve, the "x-ray image" in Figure 1 was quantitatively analyzed to determine the thickness at each pixel. The darker a pixel is; the thicker the void is associated with the inclusion. The porosity (or void fraction) at each pixel was measured. This porosity fraction was the measured porosity thickness from the "x-ray image" gray level, shown Figure 1, divided by the "sound" or nominal plate thickness, which in this case was 0.5". A map of the measured porosity fraction from the radiograph resulting from this analysis is shown in the "porosity fraction" image in Figure 1 for this x-ray. The severity of the inclusions in each experiment was quantitatively compared by summing up the total volume porosity volume, and volume percentage in each cope slice. Given that this volume percentage is missing from the nominal plate volume, here it is referred to as the "lost volume" in the radiograph. This lost volume measurement is used to summarize the severity of inclusions found in a given experiment using Method 1.

Inclusion Measurement Method 2: Quantitative Image Analysis of As-Cast Surface

Given the expense of Method 1, and the number experiments planned for this work, an alternative method of analyzing the experiment results was devised. In this concomitant inclusion measurement method, surface inspection and image analysis are performed. The inclusions on the as-cast surface are identified, as shown in the four "inclusion examples" images in Figure 2. After identifying the inclusions on the as-cast cope surface (lower left image in Figure 2), envelopes are marked and filled in at each inclusion using *Paint 3D* software as shown in Figure 2. This image can then be converted a binary format ("processed binary image" in

Figure 2). From this binary image, the area of the marked indications can be measured by the image analysis software *Fiji* [4]. Some filtering is performed as mentioned in the lower right of Figure 2. After this, the number of discrete inclusion indications, the indication size distributions, and the measured indication area fraction on the casting surfaces can be measured using this method. Some example results are given in the bottom right of Figure 2.

Inclusion Measurement Method 3: Analysis of Media Blasted Surface, “Pit Method”

This method is similar to method 2, except that the as-cast cope surface undergoes media blasting. This was performed to improve the inspection by reducing uncertainties in determining whether indications on the casting surfaces are inclusions, or if they are caused by some other casting surface phenomena (mold-metal reaction, scale, cold laps, flow lines etc.). An example of the before/after media blasting of a cope surface is shown in the two upper left images in Figure 3. It was found that the media blasted surfaces gave clear evidence of inclusions. The main identifying feature of inclusions on the casting surfaces were found to be pits, which are visible under the inclusion location after blasting the surface and removing the inclusion (see “examples of inclusion pits” images in Figure 3). Since these pits go hand-in-hand with the inclusions, they were used to identify inclusion areas on the experimental casting surfaces, and to distinguish between inclusions and other surface indications such as cold lapping and scale. The inclusion locations are marked by hand with a dot on the cope surface and then photographed (lower left image in Figure 3). The photo is digitally marked with an envelope in *Paint 3D* (lower middle image in Figure 3), and converted to the “processed binary image” as shown in Figure 3. Like Method 2, from Method 3 the number of discrete inclusion indications, the indication size distributions, and the measured indication area fraction on the casting surfaces can be measured.

Note that in Figures 1, 2 and 3, the same cope surface section has been measured by each of the three methods. The results for each method can be compared. Method 1 measures the gas byproducts and not the actual inclusions, and despite it being a completely quantitative measurement method, it is at best an indirect method of inclusion measurement. Method 3 results in smaller and more numerous inclusions than Method 2, and it gives a lower area fraction than Method 2.

Effects of Chills on Cope Surfaces of Casting Experiments

The experiments were designed so that the castings would capture any and all inclusions possible for measurement. In steel castings, inclusions can be removed from castings during filling if the flow carries them into feeders. It was determined early on in the experiment design process that feeders should be avoided for this reason. However, it was determined that without feeding the solidification shrinkage, the casting cope surface would form a sump, and suck into the casting. This made the measurements difficult. To avoid this, chill plates were used at the cope surfaces in these experiments to create a uniformly flat surface through rapid directional solidification resulting in the best material for inclusion measurement.

Two experiment cases were performed to investigate the differences and the effect of the chill plate on the measurement results. The cases consisted of the casting geometry shown in Figure 1 that were poured through the riser, with and without a cope chill plate. Images of the

two cases, their cope surfaces, and the measurements from Methods 1 and 2 are shown in Figure 4. Also at the far right in Figure 4 are shown the inclusion size distributions that were measured using Method 2. Little difference was observed in the overall inclusion size distributions. The inclusion locations in both cases appear to cluster at the feeder neck/inlet side (indicated by the thick red line) in the Method 1 x-ray analysis. The measurements by Method 2 give a similar inclusion area percentage, with the chill case having a fairly uniform inclusion distribution on the cope surface, and the no-chill case having inclusions located at the center of the cope surface. In short, the differences between the two cases are no greater than what one would see for a repeated case.

Measurements and Analysis of Inclusion Size and Shapes

It was found during the media blasting process that observed inclusions on the as-cast surface (for example Figure 5 a) would leave behind a divot in the casting surface after its removal (for example Figure 5 b, for the same inclusion). The inclusion size distributions measured on the cope surfaces of the castings correspond to this “flattened” inclusion geometry. A simple geometry that can be used to represent the observed inclusion shapes is a flat disk such as that shown in Figure 5c. However, when an inclusion is physically conceived of, and numerically modeled in casting simulations, it is considered to be a sphere [5]. By determining relationships between equivalent diameters of disk-shaped inclusions and spherical ones having the same volume (see Figure 5d), the predicted spherical inclusions resulting from models can be converted to equivalent disk-shaped inclusions observed in experiments, and vice versa. This allows for a more accurate comparison between measurement and simulation results.

A study was performed as outlined below to perform these conversions by analyzing inclusion sizes and geometries on the surfaces of casting experiments. Assuming a disk-shaped inclusion has a circular area A_{inc} , it would have an equivalent diameter d_d and thickness t that correspond to an inclusion volume V_{inc} . If the inclusion is spherical, it has a diameter d_s and the same volume V_{inc} . Inclusions were analyzed on casting surface to measure their area, thickness and equivalent disk diameter (assuming they are circular). These measurements can be compared with a spherical inclusion having the same volume. The measured equivalent diameters for the disk-shaped and spherical-shaped can be compared to determine if a relationship between them exists. The steps for doing this are outlined below.

Seven steps are outlined for analyzing the inclusion size and shape data. First an inclusion is identified and its perimeter is marked as shown in Figure 5a. Next the inclusion material is removed from the casting surface as shown in Figure 5b. Next, the depth of the inclusion on the surface is measured giving the value of the inclusion thickness t (see step 1 below). Then the inclusion area A_{inc} is measured using the image analysis software *Fiji* (step 2, listed below). The inclusion volume V_{inc} can then be calculated (see step 3 below), and the equivalent disk diameter d_d of the inclusion can be calculated (see step 4 below). Assuming a spherical inclusion of the same volume (see step 5 below), the equivalent spherical diameter d_s for the inclusion is calculated (see step 6 below). Finally, the diameter ratio R_d between the equivalent disk diameter d_d and the equivalent spherical diameter d_s for the inclusion can be calculated (see step 7 below). If a relationship between R_d and d_d or d_s is found, that relationship can be used to convert the

spherical inclusion size distribution result to a disk-shaped one, or vice versa. The steps and calculations referred to above are listed below:

1. Inclusion Thickness: t Measured value (digital indicator)
2. Inclusion Area: A_{inc} Measured value (Fiji)
3. Inclusion Volume: $V_{inc} = tA_{inc}$
4. Equivalent Disk Diameter: $d_d = \sqrt{\frac{4A_{inc}}{\pi}}$
5. Sphere Volume: $V_s = \frac{\pi}{6} d_s^3$
6. Equivalent Spherical Diameter: $d_s = \sqrt[3]{\frac{6}{\pi} V_{inc}}$
7. Diameter Ratio: $R_d = \frac{d_d}{d_s}$

The analysis method outlined above was performed on 21 inclusions on casting surfaces. Important results are plotted versus the equivalent disk diameter d_d of the inclusions in Figures 5e and 5f. In Figure 5e the measured disk thickness t increases with increasing d_d with some scatter for the 21 inclusions measured. From this, note that a curve fit can be used from the data in Figure 5e to determine the inclusion thickness from the area of the inclusion measured using the image analysis. So from the image analysis one can calculate the given volume of an inclusion. Continuing through the calculation steps above, the diameter ratio R_d can be calculated for each inclusion measured. In Figure 5f, the diameter ratio R_d ranges from 1.21 to 2.03, where R_d is plotted versus the equivalent disk diameter d_d of the inclusions measured by image analysis. The diameter ratio R_d could have been plotted versus the equivalent spherical diameter d_s for the inclusion. Either way, the average diameter ratio R_d is 1.71. Either this average value, or a curve fit from the data in Figure 5f, could be used to convert an equivalent disk diameter d_d to the spherical diameter d_s , or vice versa. A key conclusion is that the effective size d_d of an inclusion on a casting surface is about 1.7 times the size of the equivalent spherical diameter d_s of the inclusion when it forms in the liquid steel.

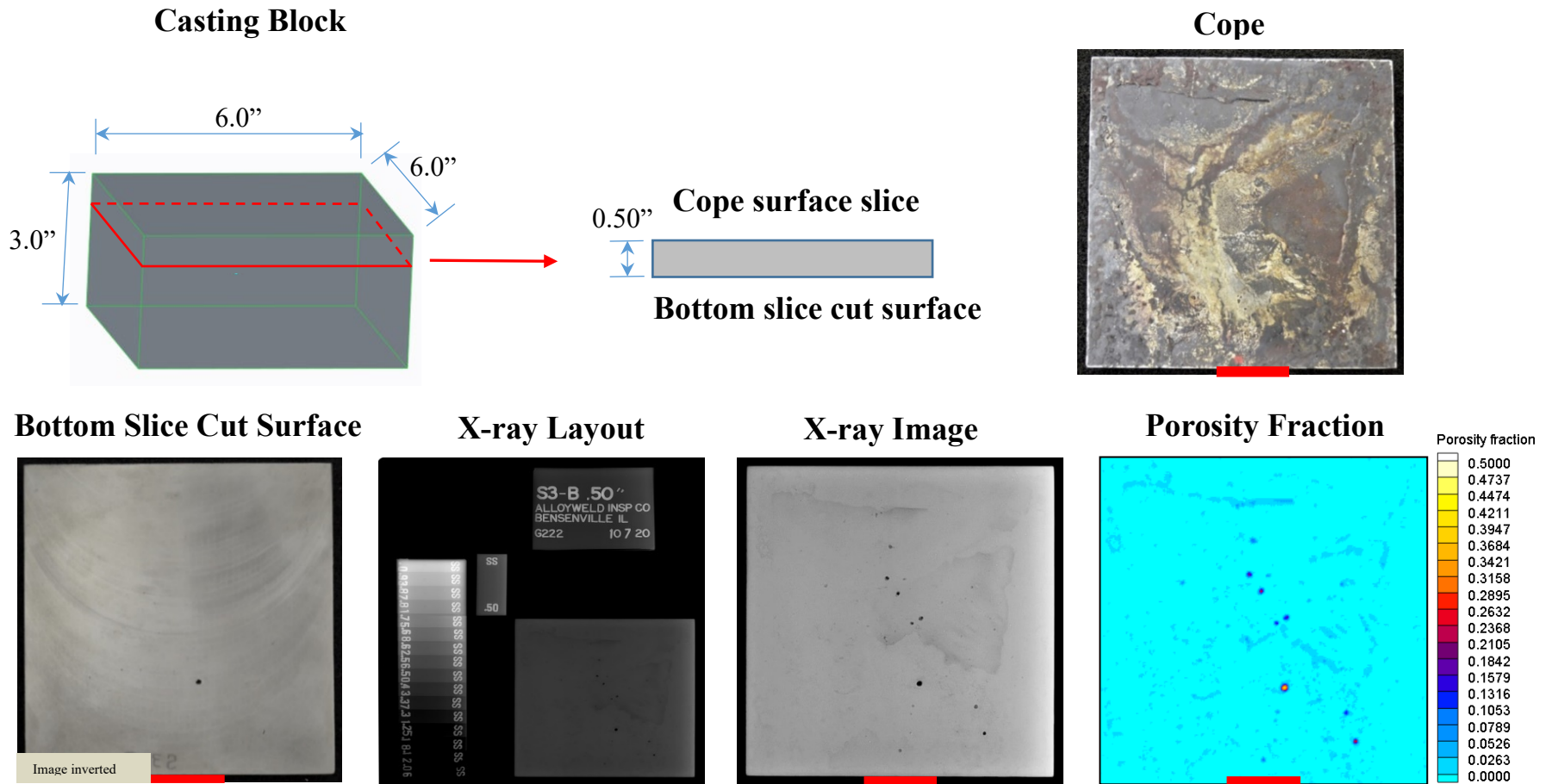
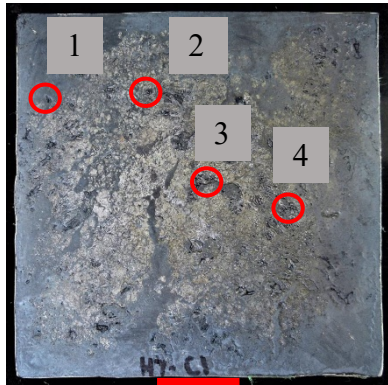
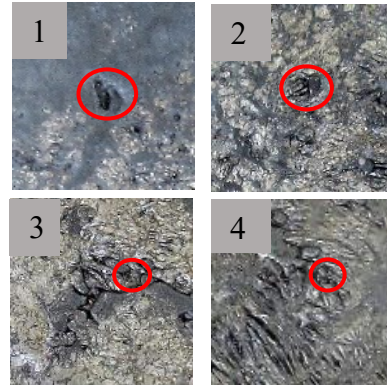


Figure 1. Images to assist the reader in understanding inclusion measurement Method 1, quantitative x-ray analysis. A cope surface slice is cut from the top of the casting and X-rayed. The gray scale image is processed to produce a % of lost volume within the slice.

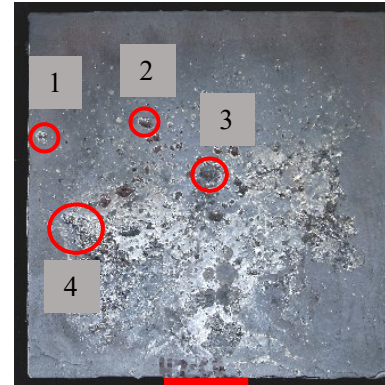
Inclusion Examples



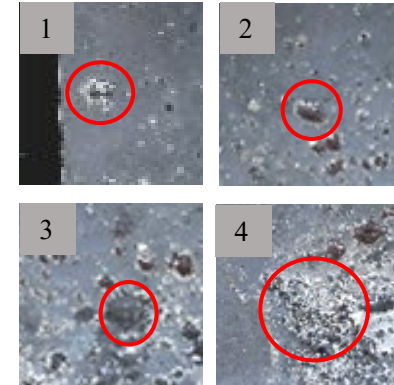
Cope Surface “As-cast”



Inclusions Marked with Paint 3D



Processed Binary Image



Processed Binary Image is:

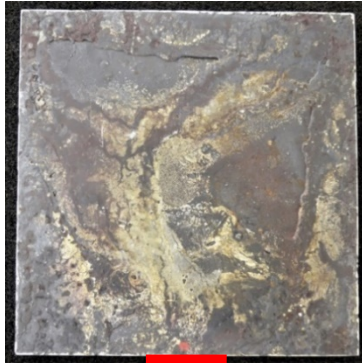
Scaled to size
 Filtered to particles $> 0.5 \text{ mm}^2$
 Calculate an inclusion count, size distribution, and inclusion area %

Example Results

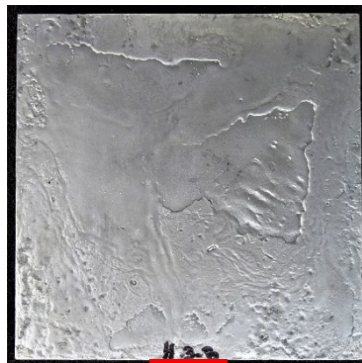
Inclusion count:	48 Inclusion
Inclusion area:	1.17%
Average diameter:	2.39 mm

Figure 2. Images to assist the reader in understanding inclusion measurement Method 2, as-cast surface analysis. The casting surface is inspected without any cleaning or preparation. Inclusion examples illustrate indications that are counted using this method. Inclusions are identified and marked. A binary image is generated and used to measure the number of inclusions, size distribution and total inclusion area % on the surface using image analysis.

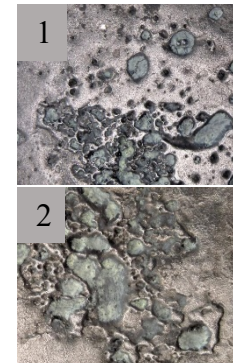
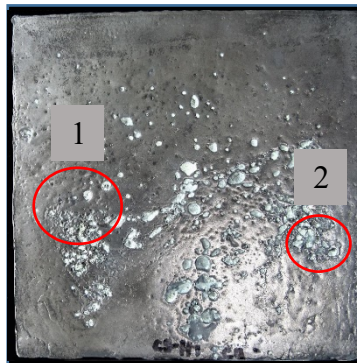
**Cope Surface
“As-cast”**



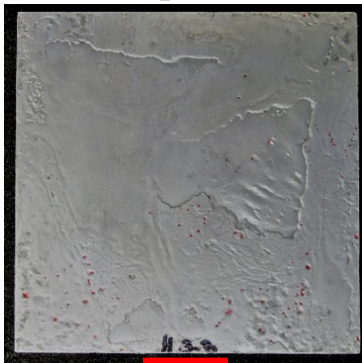
**Cope Surface
“Media Blasted”**



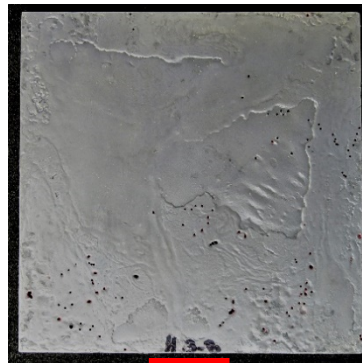
Examples of Inclusion “Pits”



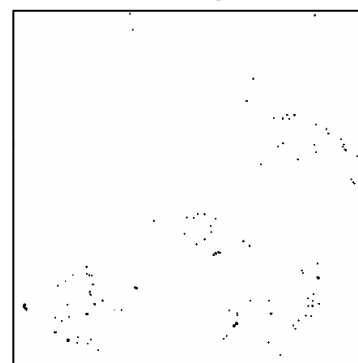
**Inclusions Hand Marked
on Cope Surface**



**Inclusions Marked
with Paint 3D**



**Processed Binary
Image**



Processed Binary Image is:

Scaled to size.
Filtered to particles $> 0.25 \text{ mm}^2$
Calculate an inclusion count,
average size and inclusion area %

Results

Inclusion count: 103
Inclusion area: 0.31%
Average diameter: 0.85 mm

Figure 3. Images to assist the reader in understanding inclusion measurement Method 3, “pit” analysis. The casting surface has been media blasted to open up surface pits before inspection. Examples of the pit indications that are counted using this method. The pits are identified and marked. A binary image is generated and used to measure the number of inclusions, size distribution and total inclusion area % of the surface using image analysis.

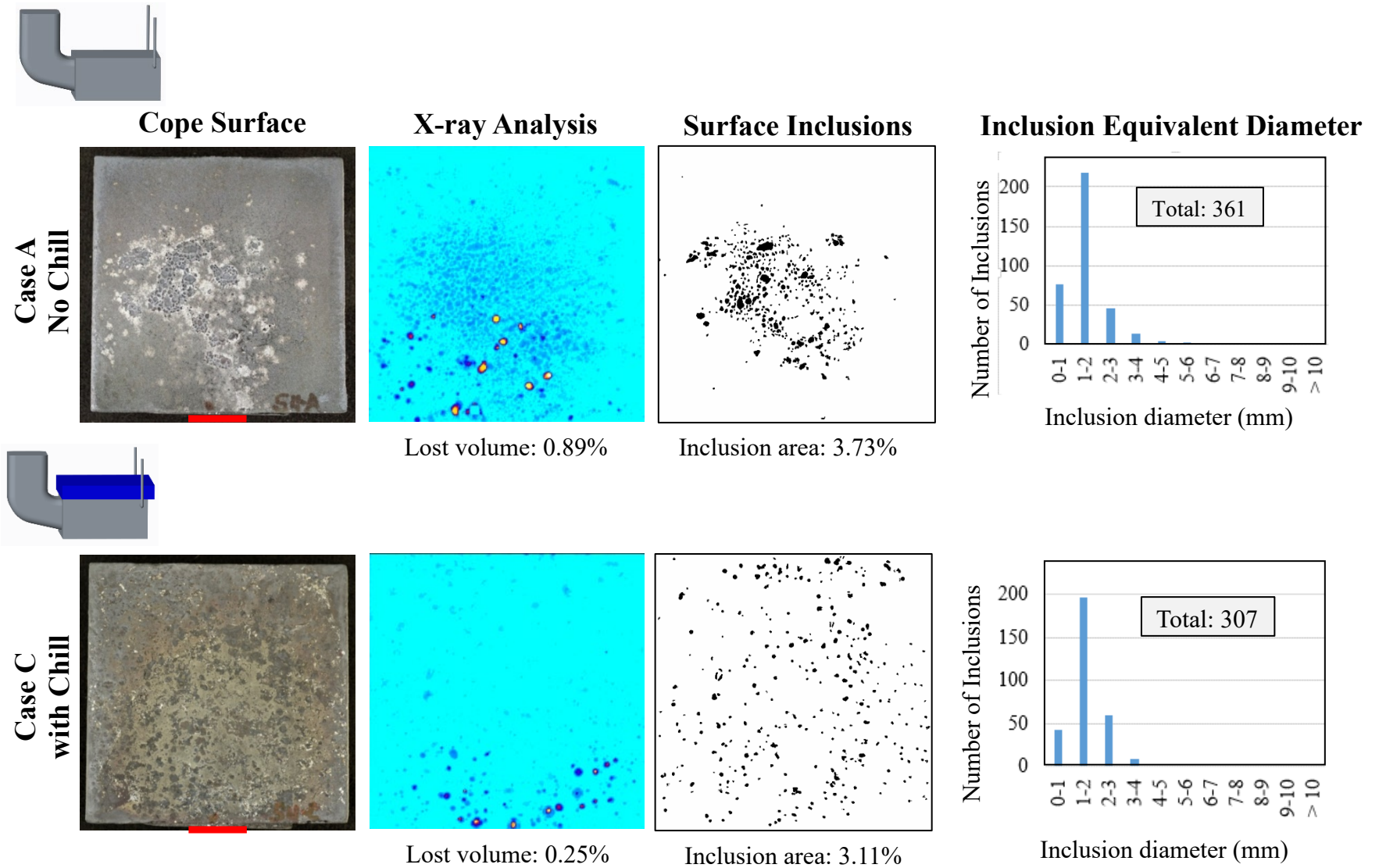
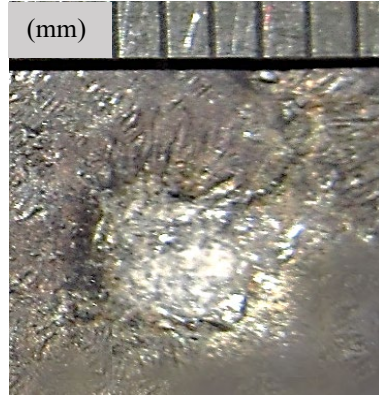


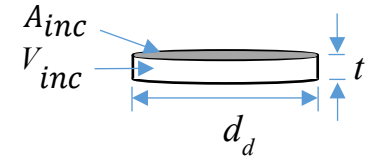
Figure 4. Images of casting cope surfaces with and without chill, and their experimental measurement results.



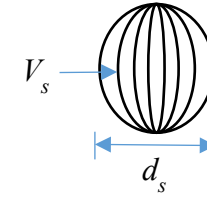
(a) Inclusion example, as cast



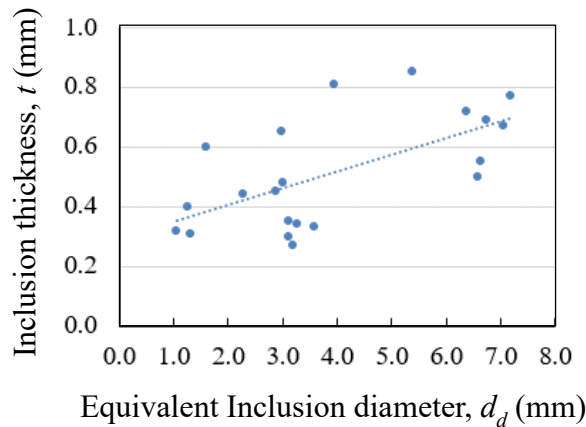
(b) Inclusion example after media blast



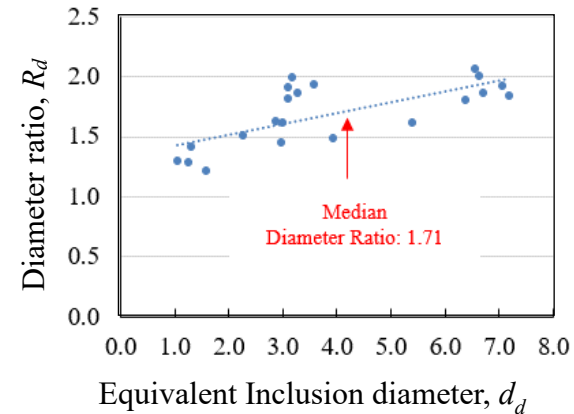
(c) Schematic of an inclusion disk



(d) Schematic of a spherical inclusion



(e) Measured inclusion thickness as a function of inclusion diameter



(f) Diameter ratio of an inclusion disk to an inclusion sphere as a function of the inclusion diameter

Figure 5. Inclusion on the as-cast surface (a) is removed leaving behind a divot in the casting surface (b) that resembles a disk (c). The disk geometry can be analyzed as an equivalent sphere (d). The analysis leads to relationships between the inclusion thickness and diameter (e), and diameter ratio and inclusion diameter (f).

Experiments Part 1: Gating System and Sprue Height Experiments and Results

Description of Gating System and Sprue Height Experiments

The effects of the gating system variables and sprue height on clean steel were investigated using the experiment cases shown in Figure 6. For the gating system study there are five fundamental cases, labeled cases A through E in that figure. Case A uses a pressurized baseline sized downsprue and ingate, and is gated into the top of the casting. Case B uses a larger non-pressurized downsprue and ingate, and it is gated into the bottom of the casting. Case C uses gating with the same dimensions as A, but with an ingate at the bottom of the casting. Case D uses a pressurized gating system with tapered downsprue and bottom filling. Cases A through D use the same pouring cup. Case E uses the same gating as Case D, except that the pouring cup is replaced by a pouring basin. Each experiment case is also poured using three different filtering conditions as shown in Figure 6 with the filter location included in the model diagrams. These cases are; no filter, filter on downsprue, and filter on runner. The three filter cases were devised to pin-point the source of inclusions. By comparing the dirt levels between the filter cases, it can be determined if inclusions come from the ladle and pouring cup, the downsprue and runner, or by the flow into the castings. All fifteen experiment cases use the same casting size and a chill plate on the cope surface.

Also shown in Figure 6 are seven cases designed to study the effect of the sprue height, or fall height, on metal cleanliness. These are cases S-A to S-D. Except for sprue height, all cases used the same gating dimensions and ingate locations. Case S-A uses the baseline sprue height with no metal filtering. Case S-B uses the baseline sprue height with a pre-filter to filter metal from the ladle before the pouring cup. Cases S-C1 to S-C4 use a filter below the pouring cup, and progressively shorter sprue heights ranging from the baseline height in case S-C1 to the shortest height in S-C4. Lastly, case S-D uses the baseline sprue height and a filter in the runner at the ingate to the casting.

Gating System Clean Steel Experiments and Results

In Figure 7 the dimensional and other information for the gating system experiments are given for the casting, chill plate, filter, pour cup and basin, downsprues, runners and ingates used in cases A to E. In Figure 8 the casting process information is given for each of the fifteen experiment cases arranged by gating system in columns, and by filtering condition/location used in rows. The process information includes; the heat number of the experiment case, the pour order (i.e. where the 2nd poured of 5 is indicated by “2/5”), pouring time, and pouring weight. The experiment results for each case, and for the three filtering conditions, are presented in Figures 9 to 13 for cases A to E, respectively. In each of these experiment result figures, the images of the casting surfaces and images of the inclusion analysis are arranged in columns for a filtering condition arranged by row. The images in the columns are; as-cast cope surface, Method 1 x-ray result, Method 2 as-cast binary map result, image of media blasted cope surface, and Method 3 binary map result. The summary results for each experiment case are shown on the left hand side of the figures under the image of the model of the case. These summary results are; the volume % of inclusions measured by Method 1 (M1), the area fraction on the cope surface

measured by Method 2 (M2), and the area fraction on the cope surface measured by Method 3 (M3).

In order to provide a comparison between the three methods used to measure the inclusions, Figures 14 and 15 are provided. These figures present images of the result of the analysis for two of the methods for comparison for all fifteen experiments. The summary results for lost volume due to inclusions or area fraction of inclusions are also provided, depending on the method used. In Figure 14 Methods 1 and 2 are compared, and in Figure 15 Methods 2 and 3 are compared. The mean inclusion diameters measured using Method 3 in the gating system experiments are given in Table 1.

The last figure of results for the gating system experiments is provided to summarize the results by inclusion measurement method as shown in Figure 16. The three plots in this figure give the total inclusion measurement for each method and case, and grouped by filter location. Without the filter the inclusions measured in the castings are significantly higher for all cases in Figure 16. Using a filter, all castings were cleaner regardless of whether the filter is at the top of the sprue or in the runner. Also, the results for the two filter location cases are the same, within the variability of the measurements. This indicates that no additional inclusions were generated in the downsprue, gating or by the metal stream entering the casting cavity. By locating filters in such a way to isolate the sources of the inclusions, it was found that the primary source of inclusions in these experiments was from the ladle and perhaps the pouring cup.

Considering the cases in Figure 16, one would expect that case A should produce a significantly dirtier casting than case E. Yet from measurement Methods 2 and 3, there is no difference between them. With reference to Figure 8 for the cases without filter, case E was poured first in the heat and case A was poured last. It is believed that pouring order might play a role in the results. The first casting poured might have significantly more inclusions coming from the ladle than later castings poured. Additional experimental trials will be performed pouring multiple castings of cases A and E in three or four heats to study the effect of pouring order. Only by having a larger number of castings can a statistically meaningful sample size to determine if and how pouring order affects the experimental results.

Regarding the measurements methods used and Figure 16, Method 1 results in about twice the lost volume measured in case D compared to case E. It is doubtful that the offset basin is better than a pouring cup by a factor of 2, as indicated by these results. This is not supported by the Methods 2 and 3 results for cases D and E. There seems to be a nice trend in the x-ray Method 1 results for cases A to C, and the increase in the measurement from C to D could be explained by falling height increasing in case D. However, Method 1 is at best an indirect measurement, since it mostly measured the gas associated with the inclusions. For the cases with and without filter, the results all cases are within the measurement variations for Methods 2 and 3. No strong conclusions can be drawn from the results other than the filter results are cleaner than no filter. Regardless of measurement method, when filters are used the metal is cleaned, and there is no way to distinguish between the cases. For the filtered cases, Method 2 measures more dirt and the variations within the cases are larger than the differences between cases, when compared to Method 3. Since Method 3 involves inspecting for inclusions on a cleaned surface,

it is the best, most trustworthy, accurate and direct measurement method for inclusions used in this study. By Method 3, without a filter there is no difference between the cases, indicating that the gating system has no effect and that any inclusions are probably coming from the ladle (or before the outlet of the pouring cup). The differences between the Method 3 results without and with filter (regardless of experiment case), also indicate the source of the inclusions is the ladle or the pouring cup.

Sprue Height Clean Steel Experiments and Results

In Figure 17 the dimensional and other information for the sprue height experiments are given for the casting, chill plate, filter, pour cup, downsprue, runner and ingate used in cases S-A to S-D. In Figure 18 the casting process information is given for each of the fourteen experiments arranged by sprue height and filtering condition/location used (in columns), and the heat number information of the experiments is given in rows. The process information includes; the heat number of the experiment case, the pour order (using the identification format from the gating system experiments), pouring time, and pouring weight.

The experiment results for each sprue height case and filter condition are presented in Figures 19 and 20 for measurement Methods 2 and 3, respectively. Method 1 was not used in these casting experiments. Images in the results figures give the inclusion analysis arranged in columns for sprue height and filter conditions, and the rows correspond to the heat number. Repeated cases are above and below one another. The images in the figures are the Method 2 as-cast binary map results in Figure 19, and the Method 3 binary map results in Figure 20. The summary results for each experiment case are given below the binary images. These summary results are; the inclusion area fraction measured by Method 2 on the cope surface in Figure 19, and the area fraction measured by Method 3 on the cope surface in Figure 20. The mean inclusion diameters measured in the seven sprue height experiments using Method 3 are given in Table 2.

In Figure 21 area fraction of inclusions measured by the two measurement methods are summarized for the sprue height experiments. In this figure it is clear that case S-A is the dirtiest, and one would expect this. It was expected that case S-D might be the cleanest, but it is not. Case S-D with the filter in the runner has quite different inclusion measurements from its results in heats 7 and 8. Note that casting S-D was poured first in heat 7, and the area fraction of inclusions measured was 2% versus 0.6% when measured from heat 8. The first casting poured in each heat is always dirty relative to cases poured later. Pouring order probably played a role in these results for case S-D. Cases S-C2 and S-C3 are consistently the cleanest castings. There might be a trend in increased cleanliness from case S-C1 to S-C2 and S-C3. However, the heat 7 result for S-C4 is quite dirty by both measurement methods. The case S-C4 heat 8 results are quite clean by both measurement methods. Case S-C4 from heat 7 is probably an outlier, and again pour order may play a role in this, as it was poured second in heat 7. With reference to Figure 18, generally speaking, castings poured earlier tend to be dirtier.

For the sprue height experiments, some additional observations are given in bullets below

- For case S-C4 measurement Method 2 appears to fail to produce good data.

- Going from case S-A to S-B to S-C1; about ½ the inclusions are filtered out coming from the ladle from S-A to S-B, and another ½ of the inclusions generated in pouring cup are filtered out from case S-B to S-C1.
- There was no effect of sprue height when a filter is used. The differences between cases S-C1 to S-C4 are no larger than the variations within a case. While sprue height did not matter, the most important factor leading to cleaner castings was the filtering out of inclusions from the ladle and pouring cup in cases S-C1 to S-C4.
- Case S-B is dirtier than cases S-C2 and S-C3, which was anticipated.
- All cases were found to have the possibility of producing cleaner castings except for cases S-A and S-B.

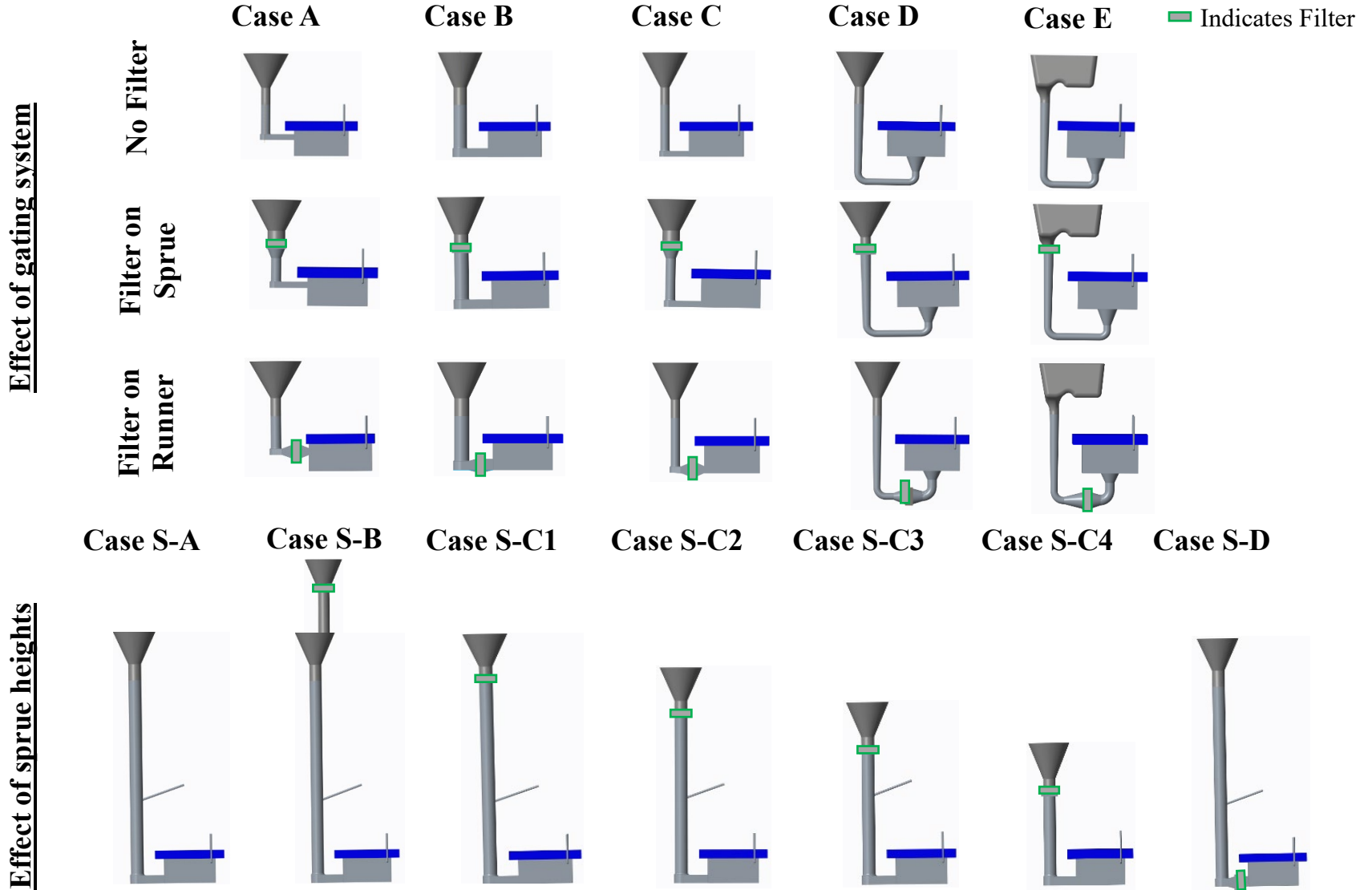
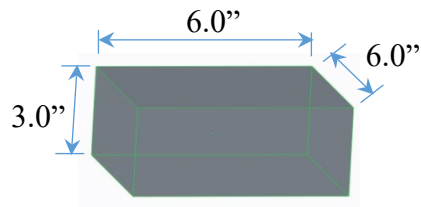
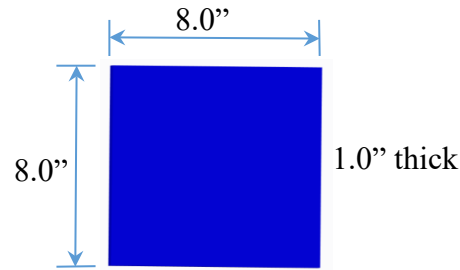


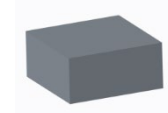
Figure 6. Cases poured in the gating system and sprue height clean steel experiments.



Casting Block

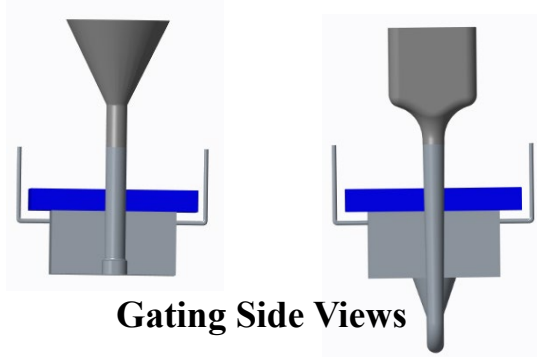


Chill Plate

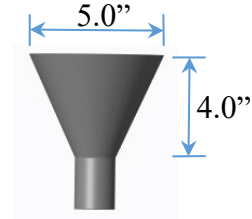


Sedex 22 – 10 ppi
Ceramic Foam Filter
2" x 2" x 0.84" thick

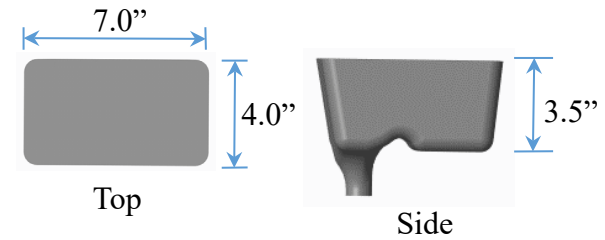
Foseco Filter



Gating Side Views



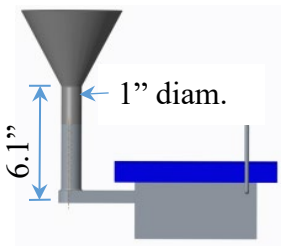
Pour Funnel



Top

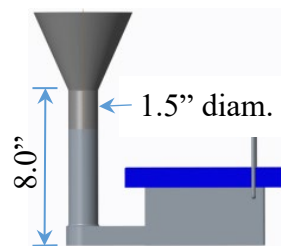
Side

Pour Basin



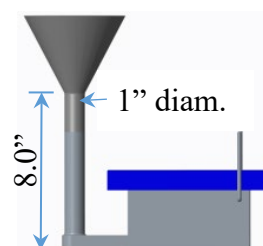
Ingate: 1.2" wide x 0.65"
Runner: 3.75" long

Case A



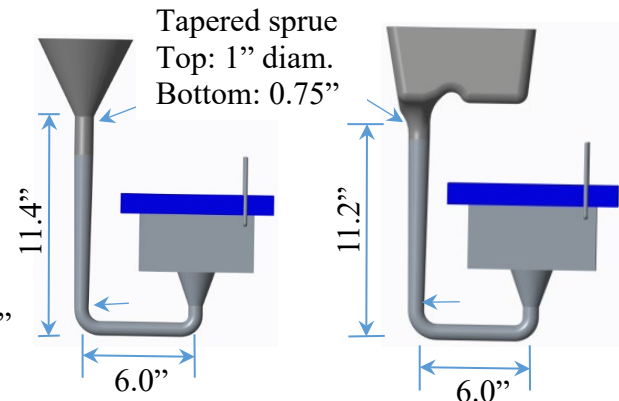
Ingate: 1.75" wide x 1.0"
Runner: 4.0" long

Case B



Ingate: 1.2" wide x 0.65"
Runner: 3.75" long

Case C



Case D

Case E

Figure 7. Dimensions and additional information for the gating system experiments for the casting, chill plate, filter, pour cup and basin, downsprues, runners and ingates used in cases A to E.

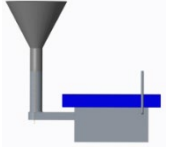
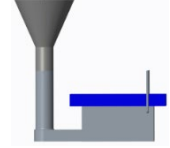
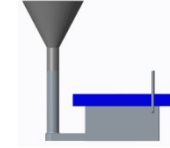
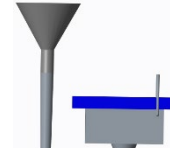

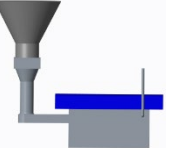
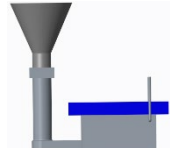
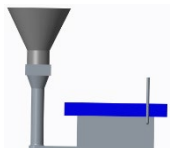
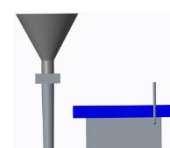
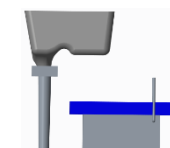
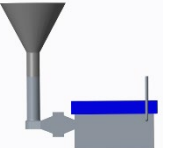
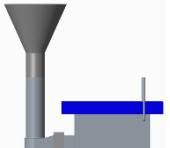
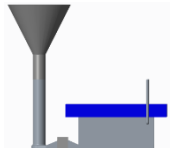
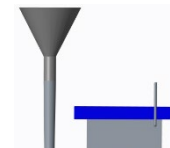
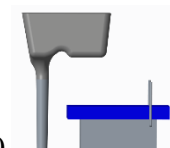
	Case A	Case B	Case C	Case D	Case E
No Filter	Heat number: 2 Pour order: 5/5 Pour time (s): 9.5 Pour weight (lbs.): 42.0 	Heat number: 2 Pour order: 4/5 Pour time (s): 10.0 Pour weight (lbs.): 46.7 	Heat number: 2 Pour order: 3/5 Pour time (s): 8.0 Pour weight (lbs.): 42.3 	Heat number: 2 Pour order: 2/5 Pour time (s): 13.0 Pour weight (lbs.): 43.5 	Heat number: 2 Pour order: 1/5 Pour time (s): 15.5 Pour weight (lbs.): 59.6 
Filter on Sprue	Heat number: 5 Pour order: 5/5 Pour time (s): 9.0 Pour weight (lbs.): 42.5 	Heat number: 3 Pour order: 2/5 Pour time (s): 14.0 Pour weight (lbs.): 47.0 	Heat number: 5 Pour order: 3/5 Pour time (s): 7.0 Pour weight (lbs.): 42.8 	Heat number: 3 Pour order: 4/5 Pour time (s): 13.0 Pour weight (lbs.): 43.8 	Heat number: 3 Pour order: 5/5 Pour time (s): 16.0 Pour weight (lbs.): 59.8 
Filter on Runner	Heat number: 5 Pour order: 4/5 Pour time (s): 7.0 Pour weight (lbs.): 42.3 	Heat number: 4 Pour order: 4/5 Pour time (s): 14.0 Pour weight (lbs.): 47.3 	Heat number: 5 Pour order: 2/5 Pour time (s): 9.0 Pour weight (lbs.): 42.6 	Heat number: 4 Pour order: 2/5 Pour time (s): 18.0 Pour weight (lbs.): 44.0 	Heat number: 5 Pour order: 1/5 Pour time (s): 13.0 Pour weight (lbs.): 60.1 

Figure 8. Casting process information for the gating system experiments cases A to E.

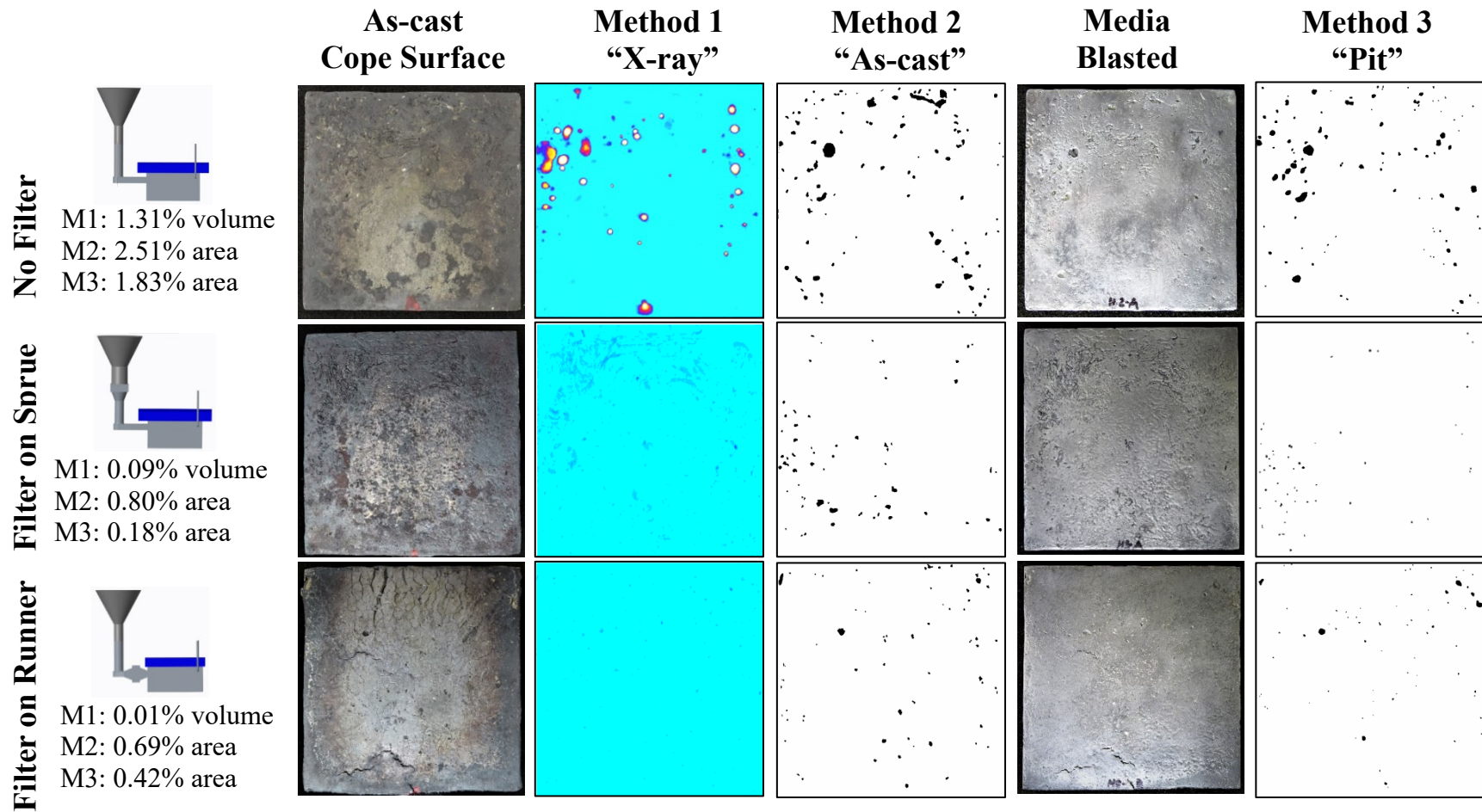


Figure 9. Measurement results and casting surface images for the gating system experiment case A.

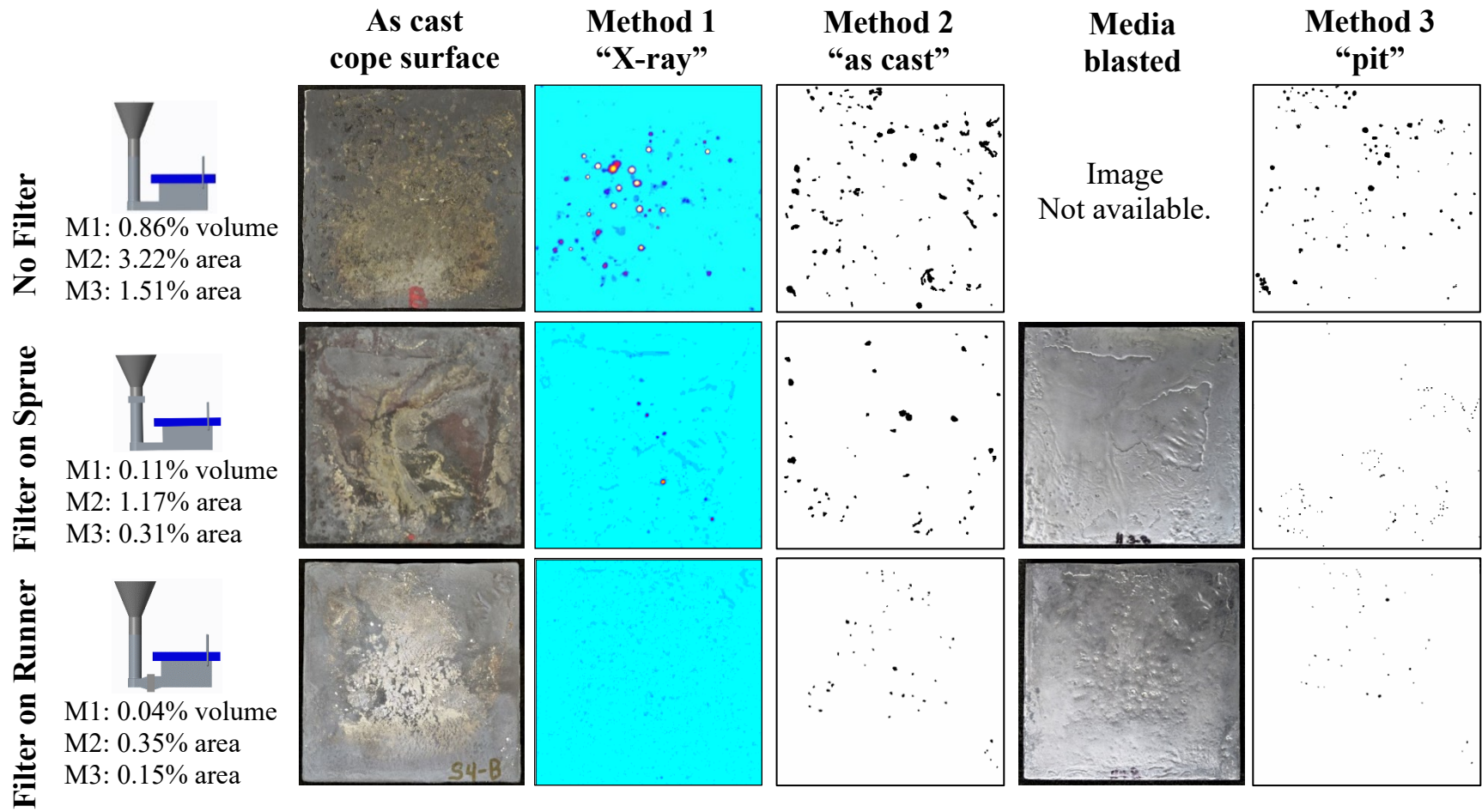


Figure 10. Measurement results and casting surface images for the gating system experiment case B.

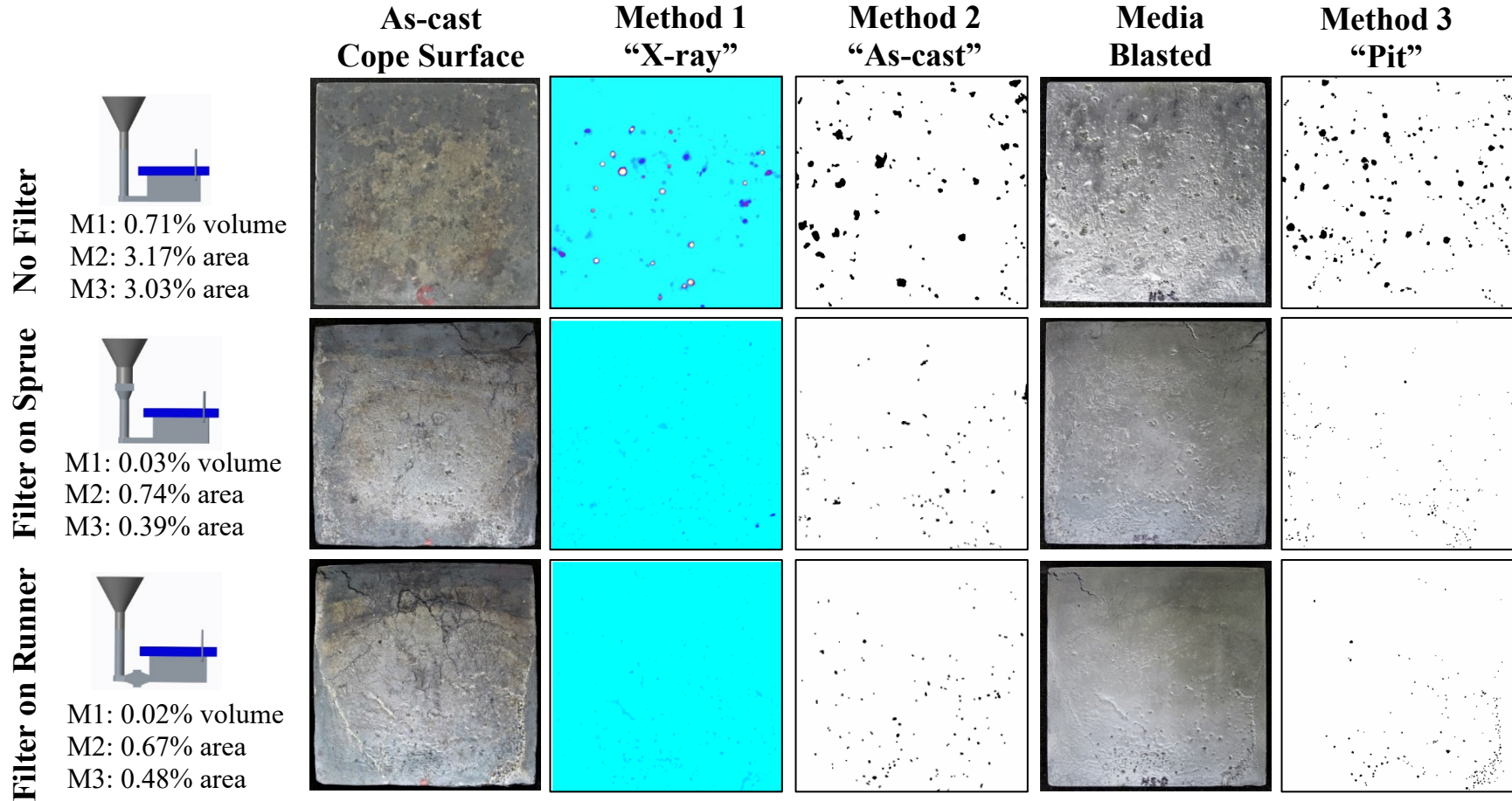


Figure 11. Measurement results and casting surface images for the gating system experiment case C.

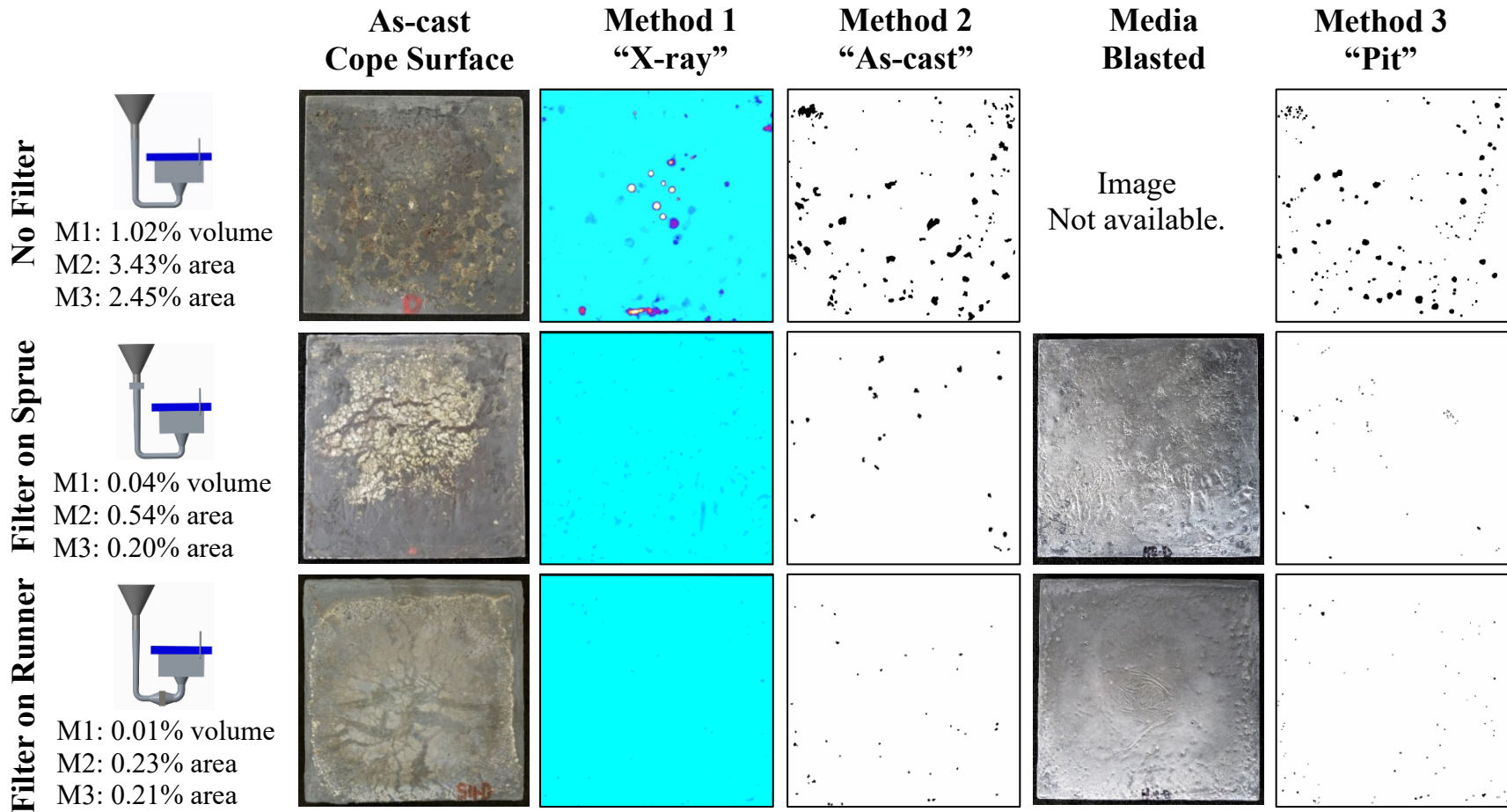


Figure 12. Measurement results and casting surface images for the gating system experiment case D.

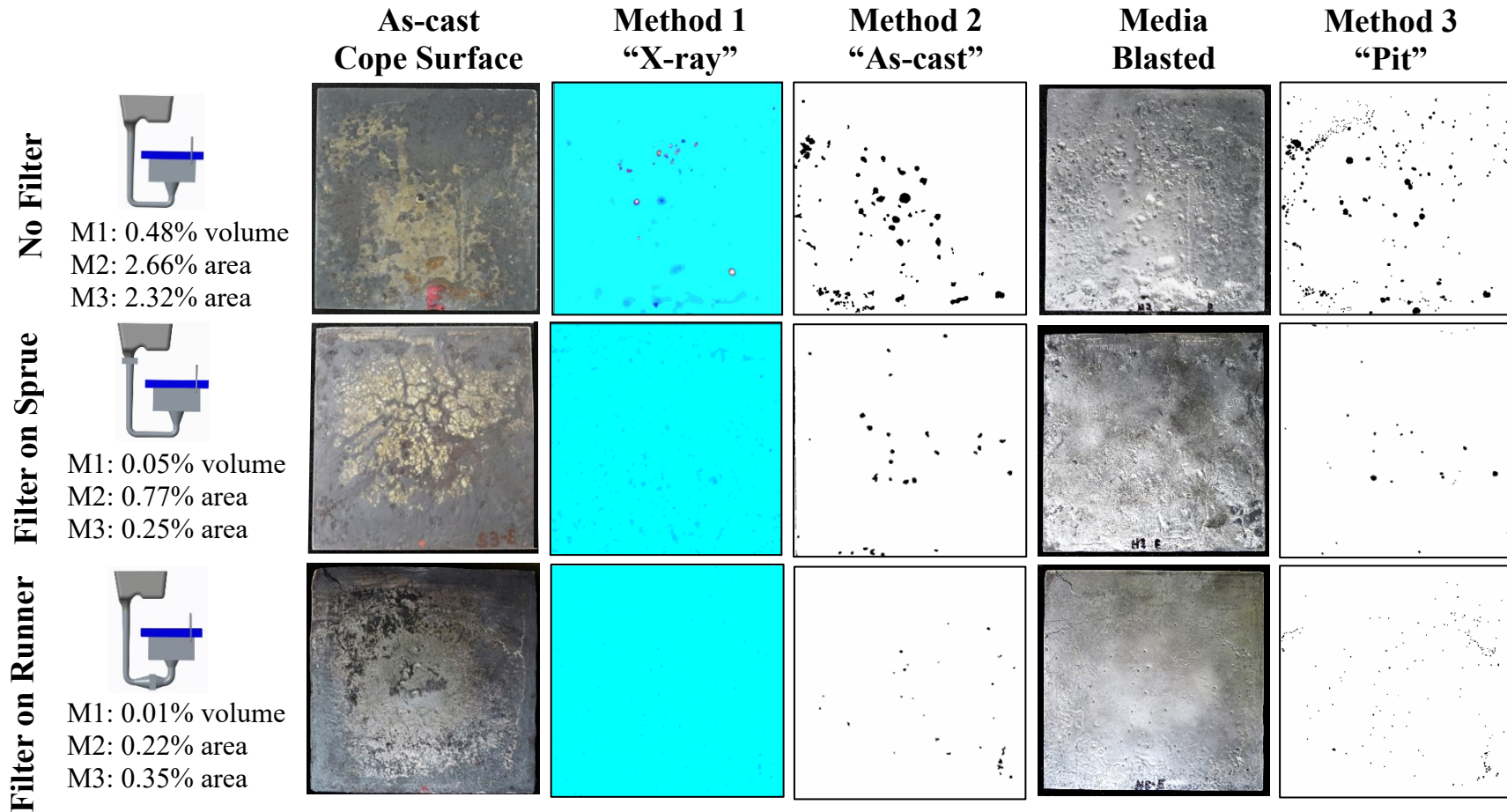


Figure 13. Measurement results and casting surface images for the gating system experiment case E.

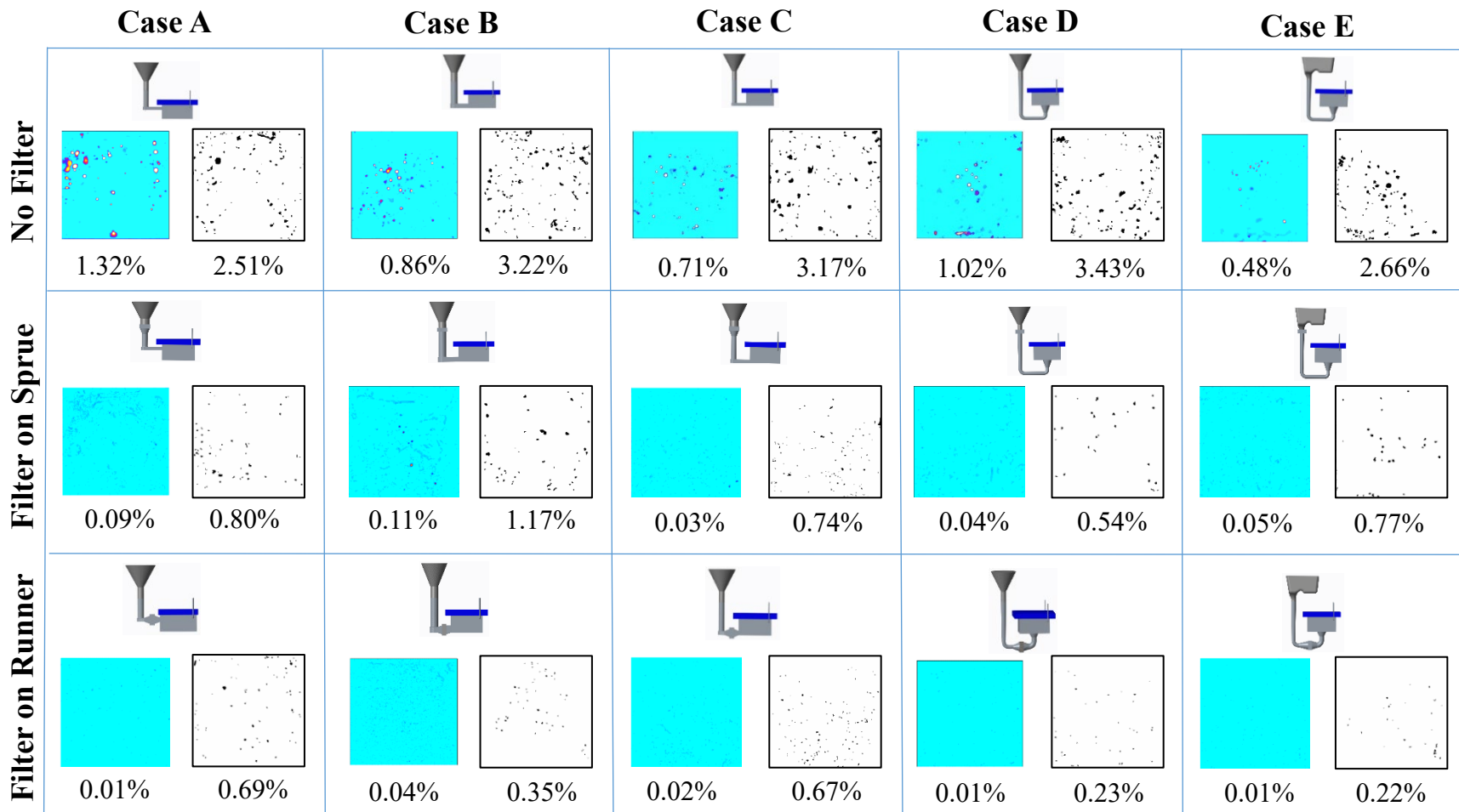


Figure 14. Gating system measurement results comparing Method 1, lost volume % is the figure on the left for each case, and Method 2, inclusion area % is the figure on the right.

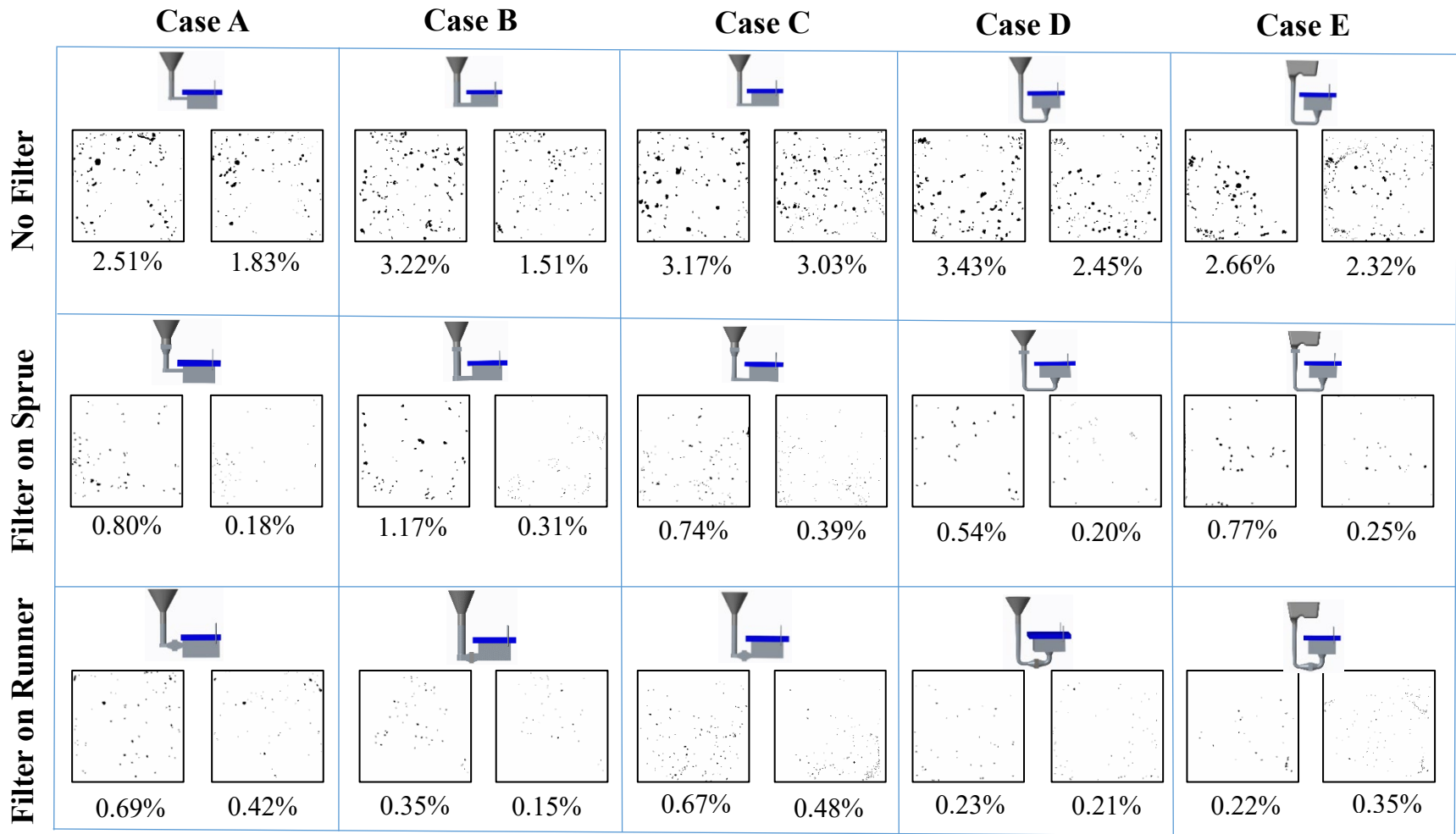


Figure 15. Gating system measurement results comparing Method 2, inclusion area % is the figure on the left for each case, and Method 3, inclusion area % is the figure on the right.

Table 1. Mean Inclusion Diameter (mm) - Gating systems summary by Method 3

	Case				
	A	B	C	D	E
No filter	2.24	1.94	1.98	2.19	1.58
Filter on sprue	0.98	0.92	0.84	1.05	1.47
Filter on runner	1.33	0.94	0.91	0.90	0.79

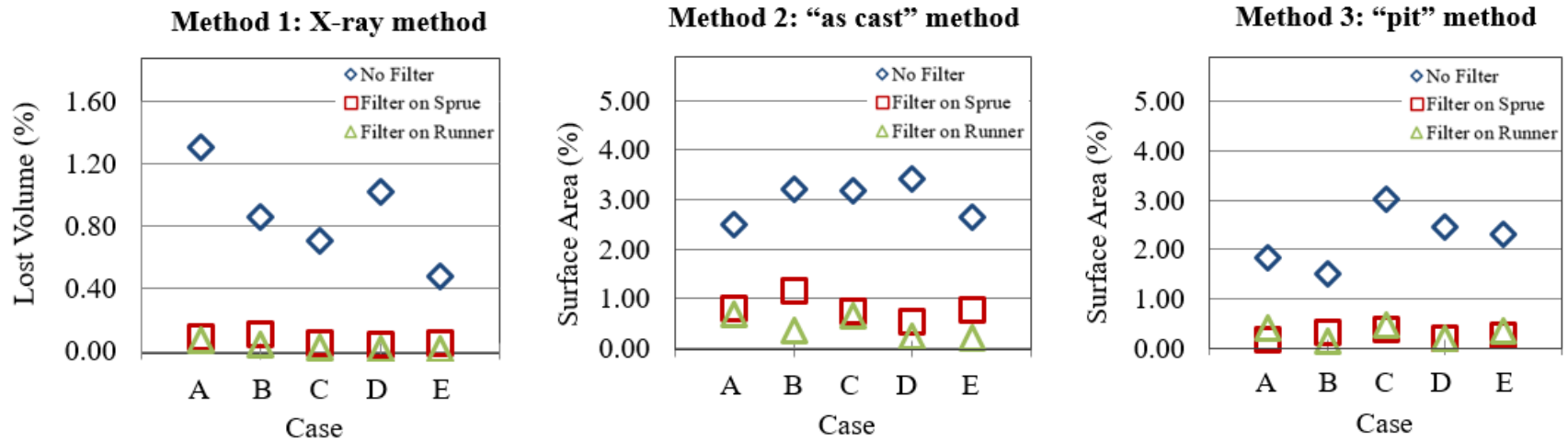
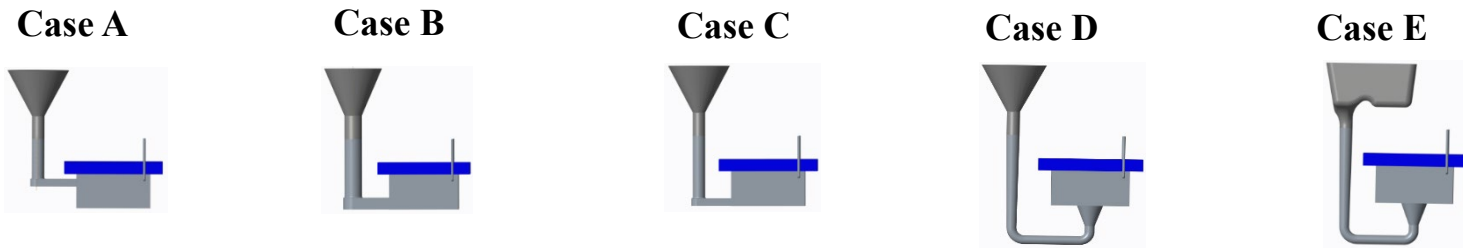


Figure 16. Summary of gating system inclusion experiment results for the three measurement methods.

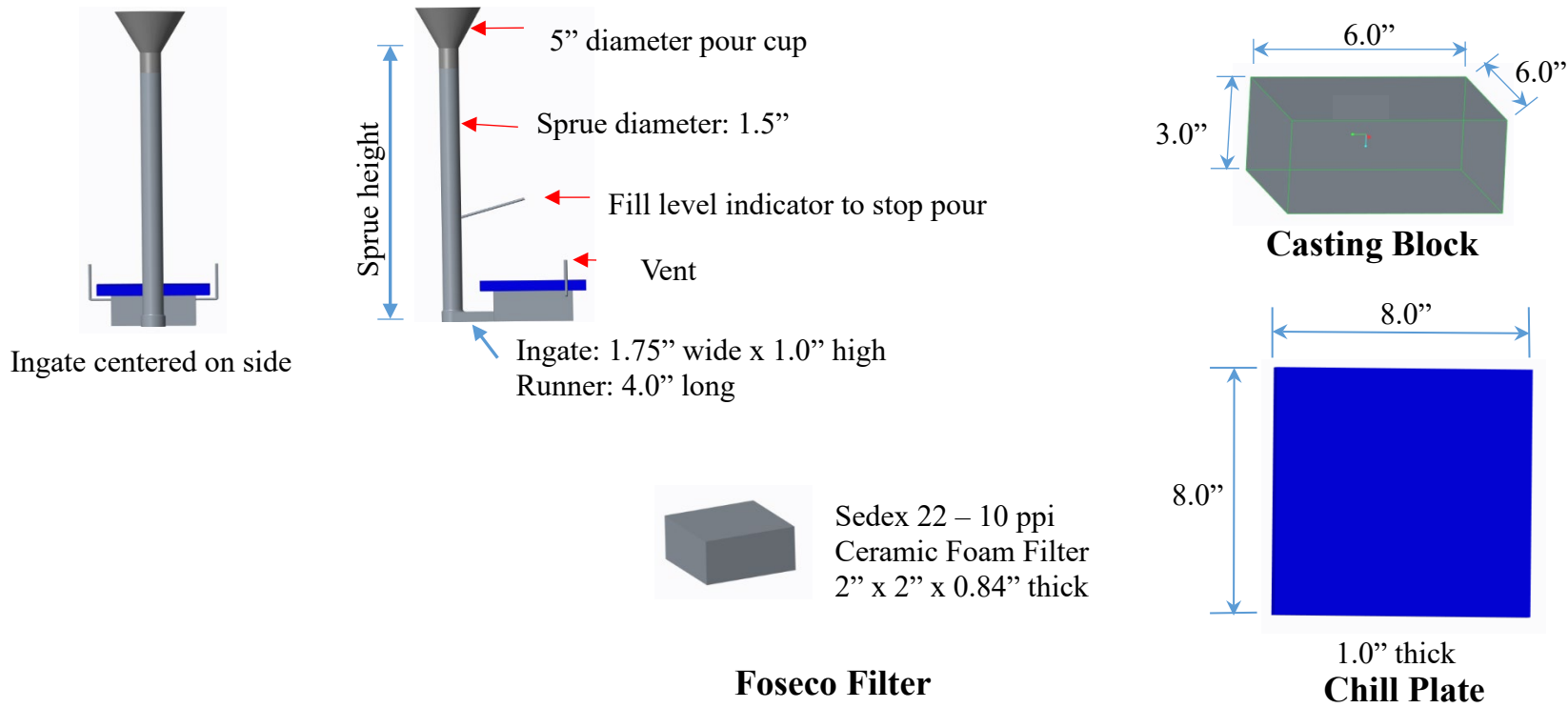
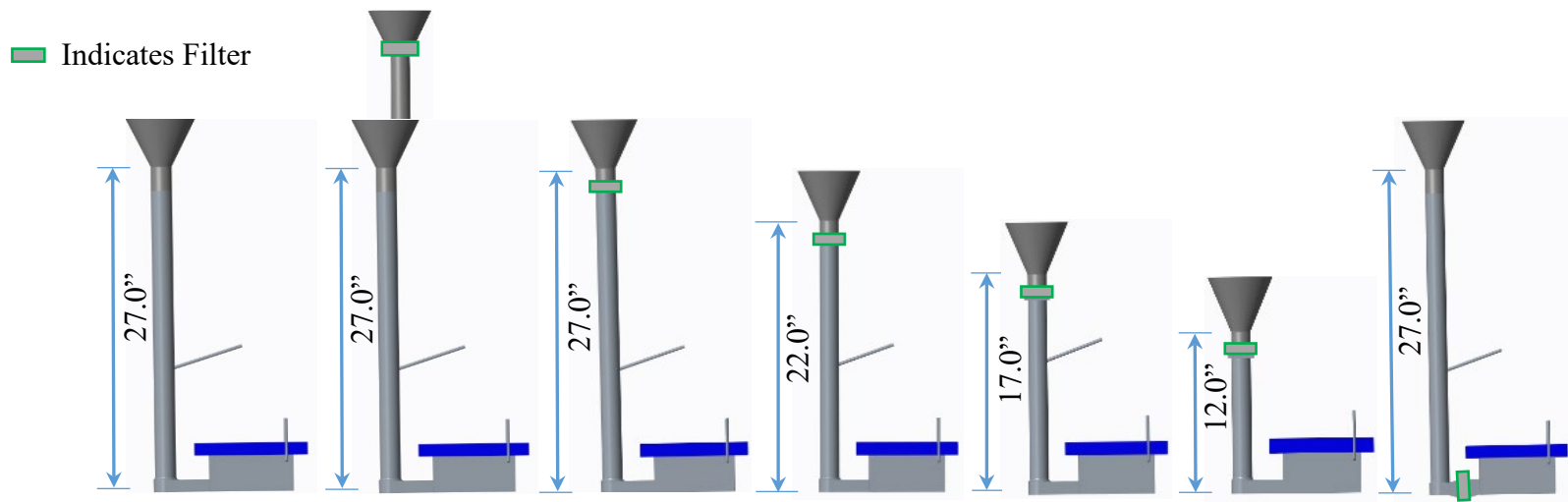


Figure 17. Dimensions and additional information used in the sprue height experiment cases for the casting, chill plate, filter, pour cup, downsprues, runners and ingates.



	Case S-A	Case S-B	Case S-C1	Case S-C2	Case S-C3	Case S-C4	Case S-D
Heat number:	6	6	6				
Pour order:	2/3	1/3	3/3				
Pour time (s):	10.0	12.0	13.0				
Pour weight (lbs.):	36.5	37.0	34.5				
Heat number:			7	7	7	7	7
Pour order:			5/5	4/5	3/5	2/5	1/5
Pour time (s):			12.0	10.0	8.0	10.0	12.0
Pour weight (lbs.):			36.0	46.5	43.0	36.5	41.5
Heat number:	8		8	8	8	8	9
Pour order:	1/5		2/5	3/5	4/5	5/5	1/3 repour
Pour time (s):	8.0		10.0	11.0	14.0	14.0	12.0
Pour weight (lbs.):	37.5		49.5	36.5	37.5	39.5	40.1

Figure 18. Casting process information for the sprue height experiment cases S-A to S-D; heat number, pour order, pour time and pour weights.

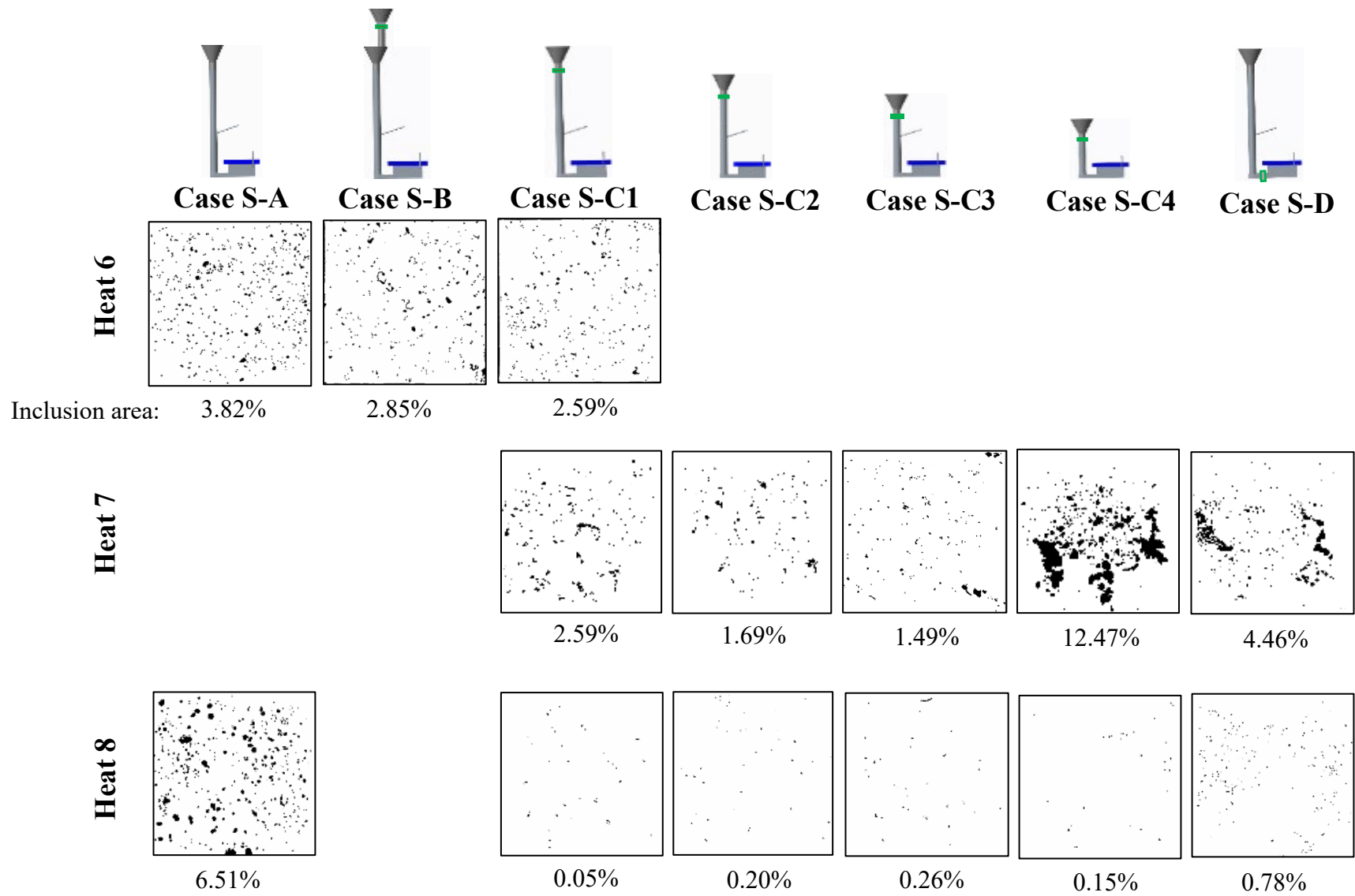


Figure 19. Sprue height inclusion experiment measurement results for Method 2, inclusion area %

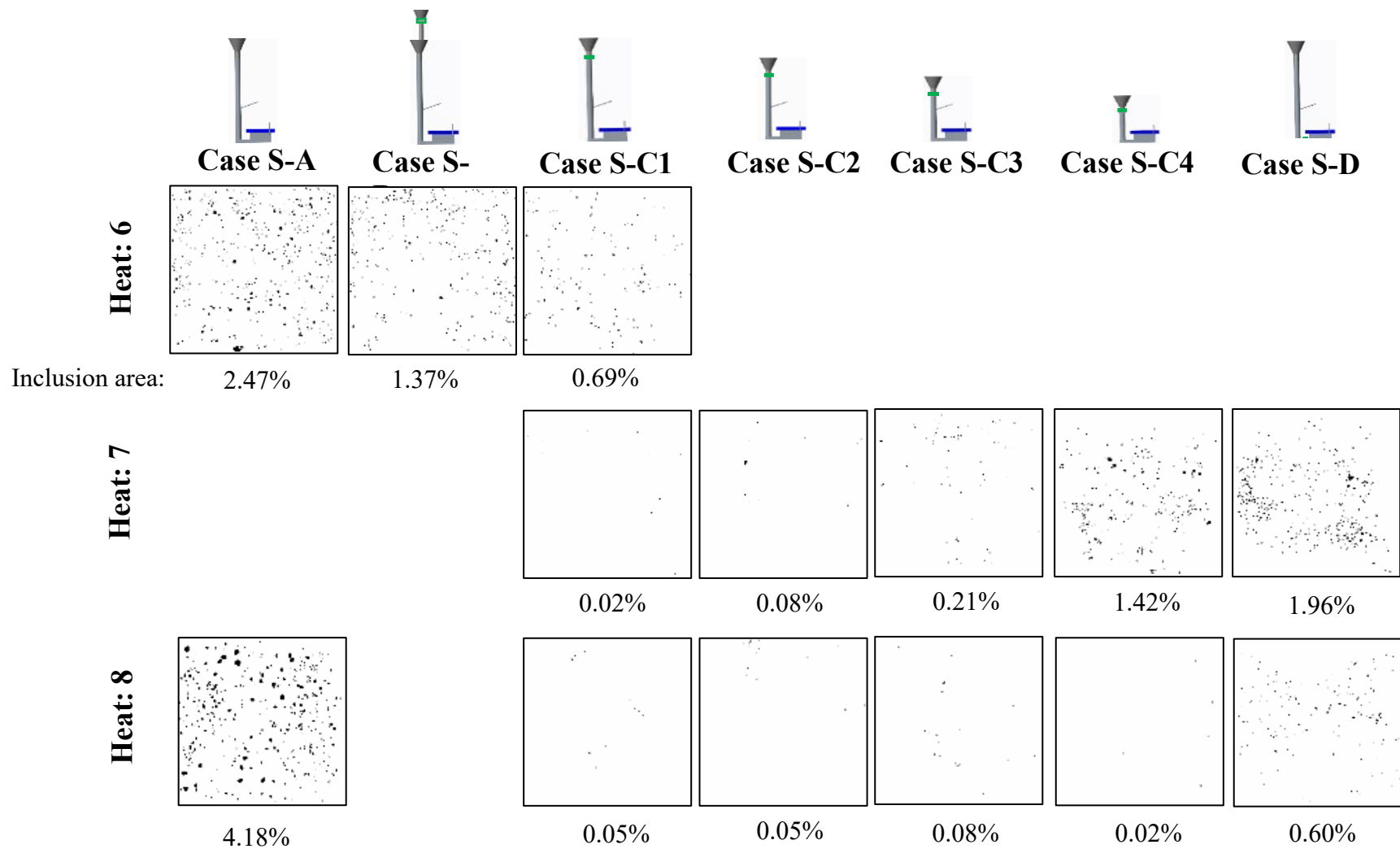


Figure 20. Sprue height inclusion experiment measurement results for Method 3, inclusion area %

Table 2. Mean Inclusion Diameter (mm) - Sprue height summary by Method 3

Case						
S-A	S-B	S-C1	S-C2	S-C3	S-C4	S-D
1.11	1.44	1.01	1.20	1.01	1.18	1.13

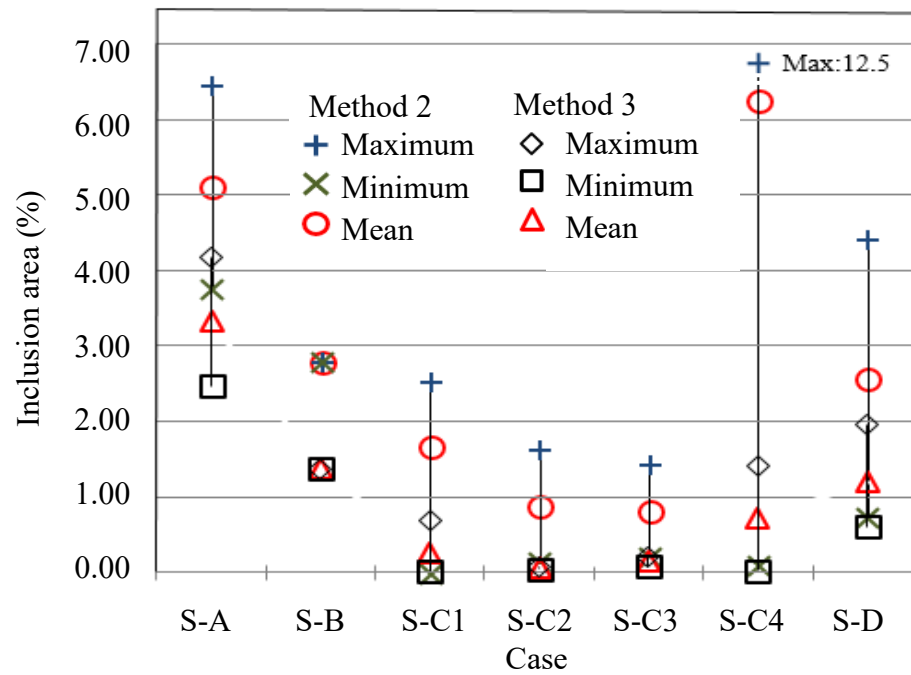


Figure 21. Inclusion area fraction measurement results for the sprue height experiment cases using Methods 2 and 3. Maximum, minimum and their mean values are shown.

Experiments Part 2: Inclusion Tracking Study Experiments and Their Results

Description of Inclusion Tracking Experiments

Three heats of inclusion tracking experiments are presented in this part of the paper. The results are presented by heats. These experiments were designed to generate inclusions and produce flow patterns to study effects of various casting geometry features on the final inclusion locations on surfaces of the castings. The inclusions in the tracking experiments were observable primarily on cope surfaces of the castings. The results of the experiments will be used to guide development and calibration of an inclusion tracking model. The castings were inspected and measured using the three methods of inclusion measurement. In heat 1 all three measurement methods were used, and in heats 2 and 3 Methods 2 and 3 were used.

As shown in Figure 22, four cases were poured in the first heat; a case with two inclined surfaces case 1-A “Angled Cope”, another with an inclined surface gated at mid-height case 1-B “Inclined Plate”, a case with flow around a circular core case 1-C, and a case 1-D with a ring flow pattern and a notch in its cope surface. The same gating and downsprue was used for all cases to control for that variability.

In the second heat of inclusion tracking experiments, two types of experiments were developed and poured. In the first type, three experiments with filling of a plate casting at three inclination angles were performed. These are shown in Figure 22 as cases 2-A, 2-B and 2-C. These cases are no inclination (or horizontal), inclined by 30 degrees and inclined by 60 degrees, respectively. These cases are similar to the "Angled cope" experiment case 1-A cast in the first heat of experiments; except the inclination angles are split into separate cases, instead of combined into one case. Note that the downsprue used is the same for all cases to avoid that variability. This downsprue height was designed to accommodate the filling of Case 2-C. Note that the same plate casting is used in the three cases so that each cope surface will have the same area, and each case the same volume. In the second type of experiments poured in heat 2, two experiments having a ring flow pattern were poured. As in the ring flow case poured in the first heat, a notch is used in one of the ring flow experiments. However, the ring was shorter and the notch slightly larger in heat 2 case 2-D than case 1-D. In the second ring flow case 2-E, a dirt trap is positioned on top of the casting. This dirt trap feature is essentially the opposite of the notch case, creating a cavity above the casting's cope surface. The notch and the dirt trap have the same dimensions.

For the third heat of inclusion tracking experiments, three inclined plate cases were poured that were nearly identical to the three plate cases poured in the second heat, except that they had no chills on their cope surfaces. This was done to provide data on whether and how the chill influences the inclusion distribution on the cope surface. These are shown as cases 3-A, 3-B and 3-C in Figure 22. Also in heat 3 two ring flow cases were poured. Case 3-E was a ring with a dirt trap (a repeat of case 2-E), and case 3-F was a ring casting with a flat top (no notch or dirt trap). More detail of the tracking experiments, and their results, are presented in separate sections for the three heats poured below.

Inclusion Tracking Experiments and Results: Heat 1

In Figure 23 the dimensional and other information for the heat 1 inclusion tracking experiment are given for the casting geometries, pour cup, downsprues, runners and ingates used

in cases 1-A to 1-D. This figure also includes the casting process information for each case. The process information includes; the heat number of the experiment case, the pour order, pouring time, and pouring weight.

The experiment results for each case are presented in Figures 24 to 27 for cases 1-A to 1-E, respectively. The experiment result figures give images of the casting surfaces and images of the inclusion analysis from the three measurement methods. The images in the figures of each experiment are; as-cast cope surfaces, x-ray image of cope section, Method 1 x-ray result, Method 2 as-cast binary map result, image of media blasted cope surface, and Method 3 binary map result. The summary results for each experiment case are shown in the figures under the image of the corresponding measurement results. These summary results are; the volume % of inclusions (lost volume) measured by Method 1, the inclusion area fraction measured by Method 2 and the inclusion area fraction measured by Method 3.

For case 1-A, shown in Figure 24, there are two cope surfaces, where cope 1 is less steeply inclined than cope 2. Note from the images of the cope surfaces there is not a great difference in their appearance. However, the radiographs and the results of the analyses of them, the more steeply inclined cope 2 section has less than half the lost volume percentage compared to the cope 1 section (0.24% compared to 0.55%). This makes physical sense as it should be more difficult for an inclusion to stick to a surface that is more steeply inclined. The inclusion locations are also biased with more inclusions on both surfaces towards the top of the casting.

For case 1-B shown in Figure 25 the section below the ingate has about twice the indication volume on the radiograph compared to the upper section (0.67% compared to 0.37% lost volume). Note that the uppermost section (above the ingate indicated by the thick red line), near the top edge of the case, is nearly clean of indications. This is the opposite of case 1-A. This is due to the flow first falling to the lower half of the plate and creeping upward as the plate fills.

For case 1-C shown in Figure 26 the total lost volume is 0.44%. The locations of the indications on the cope surface are strongly biased toward the ingate side of the casting. Clearly the flow pattern during filling carries many more inclusions to the ingate side of the cope surface. Note also the effect of the presence of the core on the inclusion distribution. The inclusions are clustered on the bottom surface of the core at its mid-length, which is essentially a cope surface for that region of the casting. The casting at the top surface of the core is remarkably clean.

In case 1-D in Figure 27 the filling flow is a counter-clockwise ring pattern, and the inclusions will circle the ring until they encounter the notch at the top of the casting and the cope surface. The notch serves as an obstacle to the flow of inclusions/dirt. No (or very few) inclusions appear on the casting surface downstream of the notch. This is section 3 of the x-ray image shown in Figure 27, and upstream of the dirt trap is section 1 of the x-ray a large amount of inclusion lost volume is measured (the largest of any section analyzed, 1.17%). The lost volume measured in section 3 for this case is the lowest measured for any section in these experiments, 0.14%. This experiment, and the other tracking experiments, should provide good range of conditions and data allowing us to improve the inclusion motion and tracking model.

Inclusion Tracking Experiments and Results: Heat 2

Dimensional and other information for the heat 2 inclusion tracking experiments are given in Figure 28 for the casting geometries, pour cup, downsprues, used in cases 2-A to 2-E. The runner

and ingate dimensions are the same as those from heat 1. This figure includes the casting process information for each case, including; the heat number of the experiment case, the pour order, pouring time, and pouring weight. Three plate castings and two ring-shaped castings were poured in heat 2.

Each plate casting weighed 35.3 lbs, and the total casting and rigging weighed 55.4 lbs. The plates in heat 2 were similar to the one cast in heat 1 except with the following changes:

- plate lengthened from 10" to 14"
- plate thickness reduced from 2.6" to 1.5" thick
- added different incline angles
- sprue height for all based on 60 degree model.

The two ring-shaped experiments poured in heat 2 are shown in Figure 28. Dimensions and the configurations shown in the figure demonstrate that one ring had a notch (recessed section) in its cope surface, and the other had a dirt trap (raised section) on the cope. The experiments were similar to the notched ring casting poured in the heat 1 experiment except that:

- ring height was reduced from 5" to 3"
- outer diameter increased from 9" to 11"
- inner diameter was increased from 5" to 7"
- the dirt trap case was added
- notch depth is still 0.5" but width changed from 1.0" to 2.0" to match the dirt trap dimensions.

The experiment results for heat 2 cases 2-A, 2-B and 2-C are presented in Figure 29. Results for ring flow experiment cases 2-D and 2-E are shown in Figure 30. In each experiment result figure, images of the casting surfaces and images of the inclusion analysis are from inclusion measurement Methods 2 and 3 are shown. Images in the figures for each experiment provided are; as-cast cope surfaces, Method 2 as-cast binary map result, image of media blasted cope surface, and Method 3 binary map result. The summary results for each experiment case are shown in the figures under the binary image of the corresponding analysis results. Summary results are the inclusion area fraction measured by Method 2 and the inclusion area fraction measured by Method 3.

Cope surface binary inclusion maps for the three plate castings and percentage of area coverage of the inclusions for each case are given in Figure 29. For the horizontal plate the inclusion locations appear clustered near the inlet (thick red line), the middle region of the plate has relatively few inclusions by Method 2. At the end of the plate there is a clustering of inclusions in a U-shape distribution by Method 2. Method 3 gives a more uniform distribution of inclusions. In both measurement methods, the horizontal plate corners are fairly free of inclusions. The inclusions in the tilted plates are biased towards the bottom/inlet end of the plate. For case 2-B, the plate horizontally inclined by 30 degrees filled by an ingate at the bottom edge. Results from both measurement methods the binary images in Figure 29 indicate the top end of the plate is free of inclusions. The inclusions for case 2-B appear to be collected in a region forming an "U" shaped front around the ingate with the base of the "U" at about the mid-height of the plate. The plate tilted at 60 degrees has the lowest level of observed inclusions by both measurement methods, and while inclusions are clustered near the inlet, there are additional

areas of inclusions higher up the plate toward the top end. The percentage of plate surface area with inclusion indications is given in Figure 29 for each case. Generally the inclined plates had fewer inclusions at the upper end (far from the inlet) compared to the horizontal plate.

For the ring castings, the binary inclusion maps and measured area surface coverage by inclusions are given in Figure 30. Case 2-D with the notch was found substantially more inclusion indications than the case with the dirt trap, 31% versus 3% surface area coverage by inclusions, respectively. In heat 2 both the notch and the dirt trap cases appear to have fewer inclusions upstream of those features. This is truer for the dirt trap, where there are almost no inclusions upstream of the feature. For case 2-D the clustering of inclusion downstream of the notch is opposite to what was observed for the notch case 1-D.

Inclusion Tracking Experiments and Results: Heat 3

In the third heat of inclusion tracking experiments the same plates were poured as in the second heat of experiments, except these plate experiments had no chills on their cope surfaces. This set of experiments was performed to investigate whether the chill influences the inclusion distribution on the casting cope surface. Dimensional and other information for the heat 3 inclusion tracking experiments are given in Figure 31 for the casting geometries, pour cup, downsprues, used in cases 3-A to 3-F. There was no notched ring poured. The runner and ingate dimensions are the same as those from heats 1 and 2. In this figure the casting process information is given for each case. The process information includes; the heat number of the experiment case, the pour order, pouring time, and pouring weight. Three plate castings and two ring-shaped castings were poured in heat 3. The ring castings cases had a dirt trap and a flat top for case 3-F.

The experiment results for the heat 3 cases 3-A, 3-B and 3-C are presented in Figure 32. The results for ring flow experiment cases 3-E and 3-F are shown in Figure 33. In each experiment result figure, images of the casting surfaces and images of the inclusion analysis are from inclusion measurement Methods 2 and 3 are shown. Images in the figures for each experiment provided are; as-cast cope surfaces, Method 2 as-cast binary map result, image of media blasted cope surface, and Method 3 binary map result. The summary results for each experiment case (inclusion area fraction) are shown in the figures under the binary image of the corresponding analysis results.

Comparing the heat 3 horizontal plate casting (no cope chill) to the analogous heat 2 casting, the inclusions are uniformly distributed throughout the middle of the plate in both cases. For cases 3-B and 3-C, the upper part of these cope surfaces are clean and inclusions are distributed toward the lower end of the plate. This was also observed in heat 2 for the inclined plates. Regardless of whether the chill is used the inclusions collect at the cope surface when they enter and as the front of metal fills the castings they stick to the cope surface. As the filling progresses the front of metal becomes cleaner. This biases the locations of the inclusion to the inlet side of the plate. There does not appear to be any systematic trend that plate inclination angle effects the amount of dirt in the castings, since the flat and steepest inclined plates have the largest area fractions of inclusions.

For the dirt trap case in heat 3 (3-E), the cope surface is clean upstream of the trap; as it was in case 2-E. There is dirt in case 3-E downstream of the trap, and it appears a bit further

downstream of the trap than for case 2-E. For case 3-F, the flat topped ring, there appears to be blobs of inclusions in the 2 to 3 o'clock position. Other than that the surface is relatively clean. It is difficult to gather much more for this one experiment. An additional experiment would need to be performed for case 3-F to see if this result is repeatable.

Summary of Inclusion Tracking Experiment Results

To summarize results from the inclusion tracking experiments, the data generated will be used to calibrate and validate an inclusion generation and tracking model. The experimental results by themselves demonstrate the effects of various casting geometric features on the final locations of inclusions in castings. Some of the main observations of the tracking experiment results are

- For a block casting with two differently inclined cope surfaces, inclusions were located at the upper ends of the surfaces at the “peak of the casting.” The lower part of the casting was much cleaner by comparison.
- For an inclined plate casting with ingate at the mid-height, inclusions were located on the cope surface on the lower half and center portion of the casting. The top end of the cope surface was much cleaner.
- For a block casting with a horizontal core, a large amount of inclusions collected on the cope surface at the core (bottom side of core) with the inclusions clustered at the mid-length of the core. The drag side at the core (top surface of the core) was entirely clean. On the cope surface of the block, the inclusion locations were located mostly on the ingate side of the casting.
- For one ring casting with a notch, inclusions were clustered upstream (in front) of it, and the surface was clean downstream of it. For the ring castings in the second heat, both the dirt trap and the notch cases were cleaner upstream of the features. The dirt trap was found to have a cleaner surface than the notch case.
- For the horizontal plates cast with and without cope chills, inclusions were uniformly distributed over the cope surfaces.
- For plates inclined at 30 and 60 degrees, with and without cope chills, inclusions were clustered on the lower half of the cope surface. The upper surfaces of the plates were relatively clean by comparison.

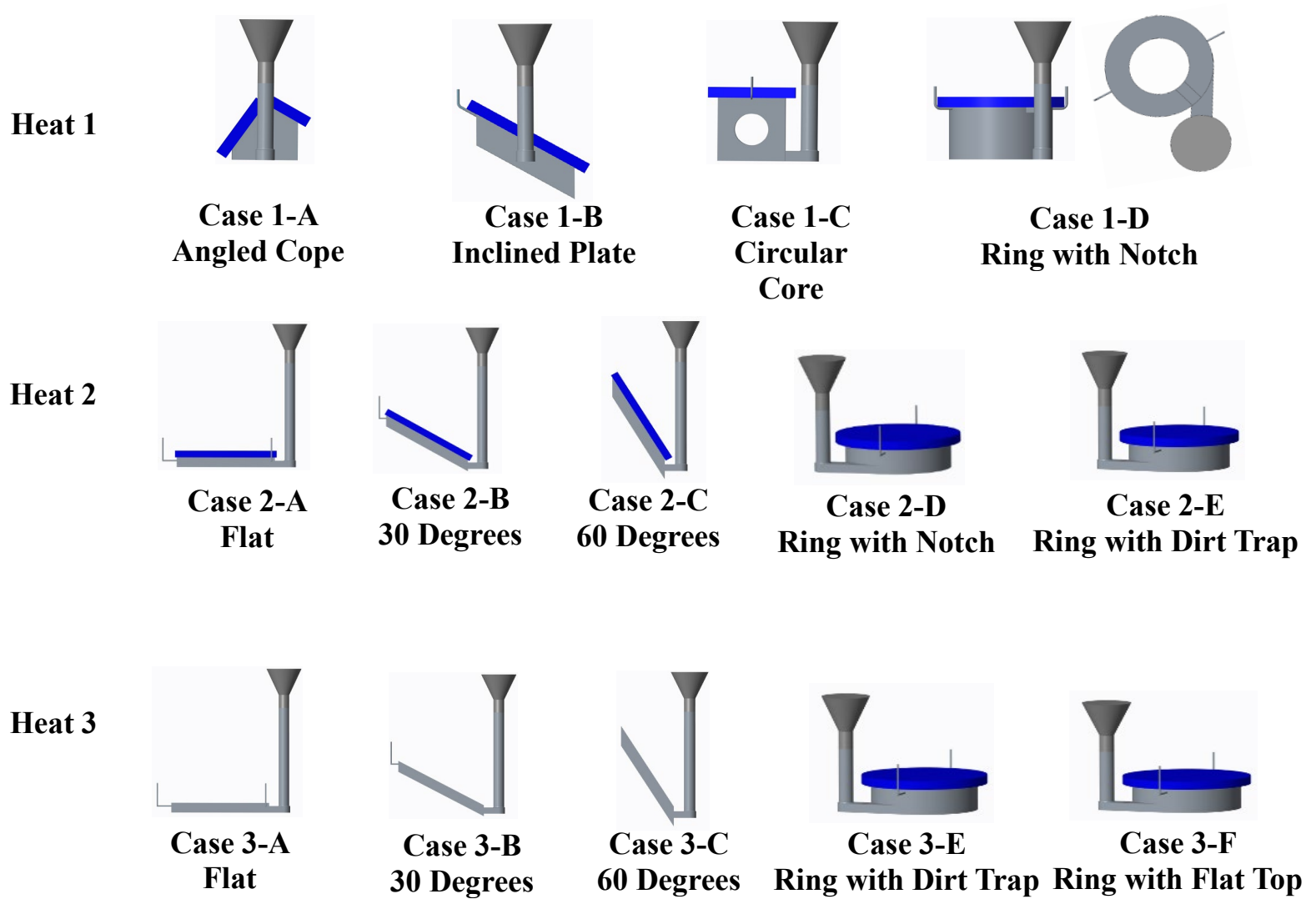
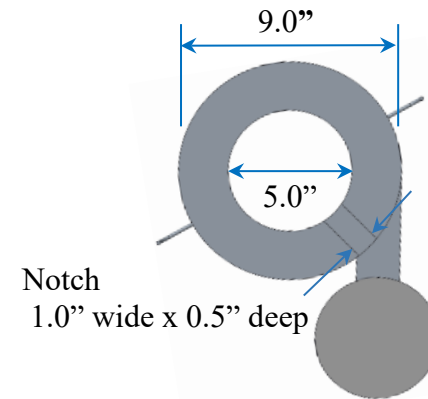
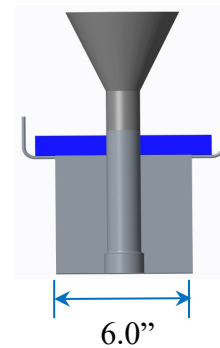
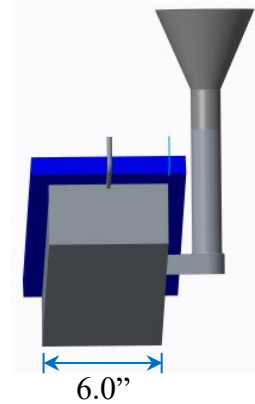
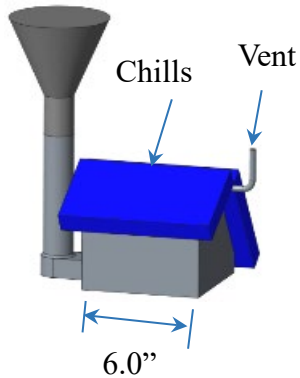
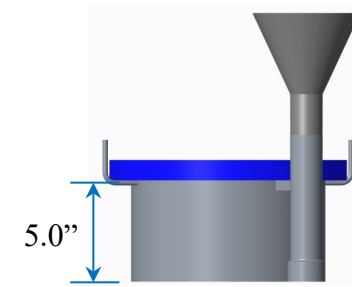
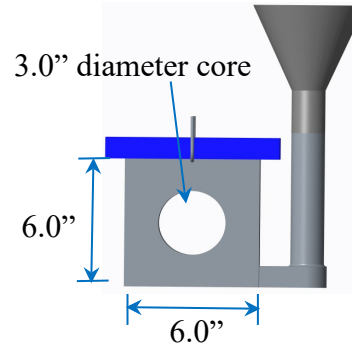
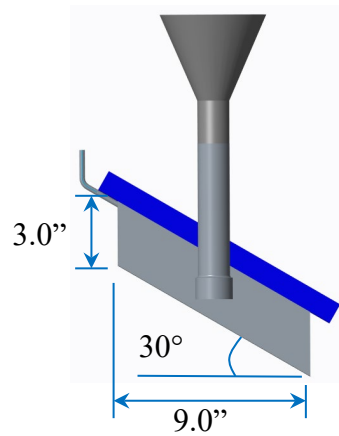
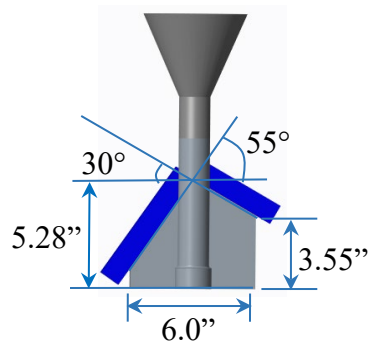


Figure 22. Cases poured in the inclusion tracking clean steel experiments.



**Case 1-A
Angled Cope**

**Case 1-B
Inclined Plate**

**Case 1-C
Circular Core**

**Case 1-D
Ring**

Processing information	Case 1-A	Case 1-B	Case 1-C	Case 1-D
Heat number:	1	1	1	1
Pour order:	1/4	2/4	3/4	4/4
Pour time (s):	10.5	15.0	11.0	12.5
Pour weight	54.1	61.0	65.2	78.7

All Cases

- 1.5" Straight sprue
- Rect. Ingate: 1.75" wide x 1.0" tall
- Gating: 1:1:1
- Pour cup: 5" top x 4" tall
- Sprue height: 9.25"

Figure 23. Dimensional and casting process information for heat 1 inclusion tracking experiment cases.

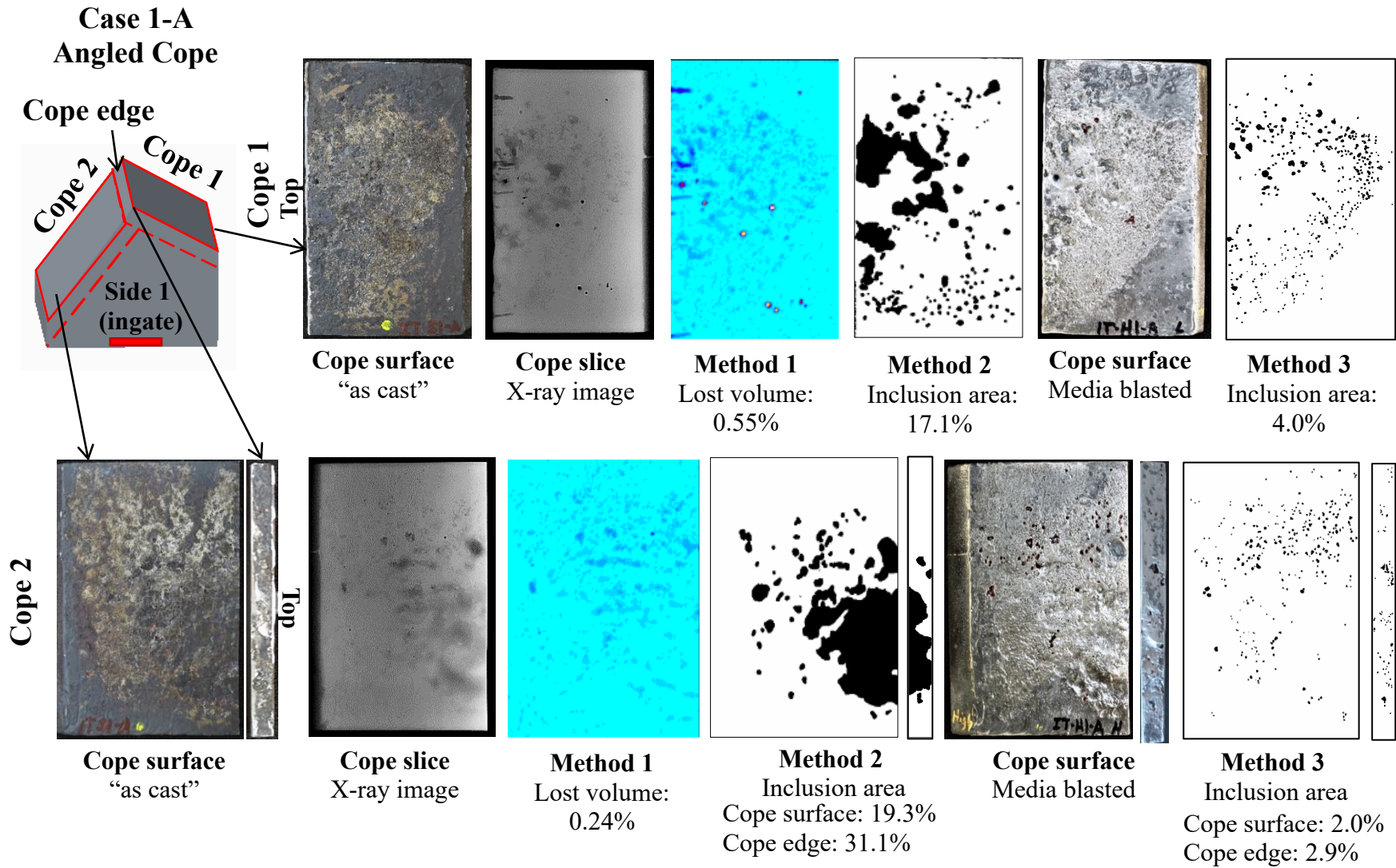


Figure 24. Images of casting surfaces and measurement results for Case 1-A using Methods 1, 2 and 3 from heat 1.

**Case 1-B
Inclined Plate**

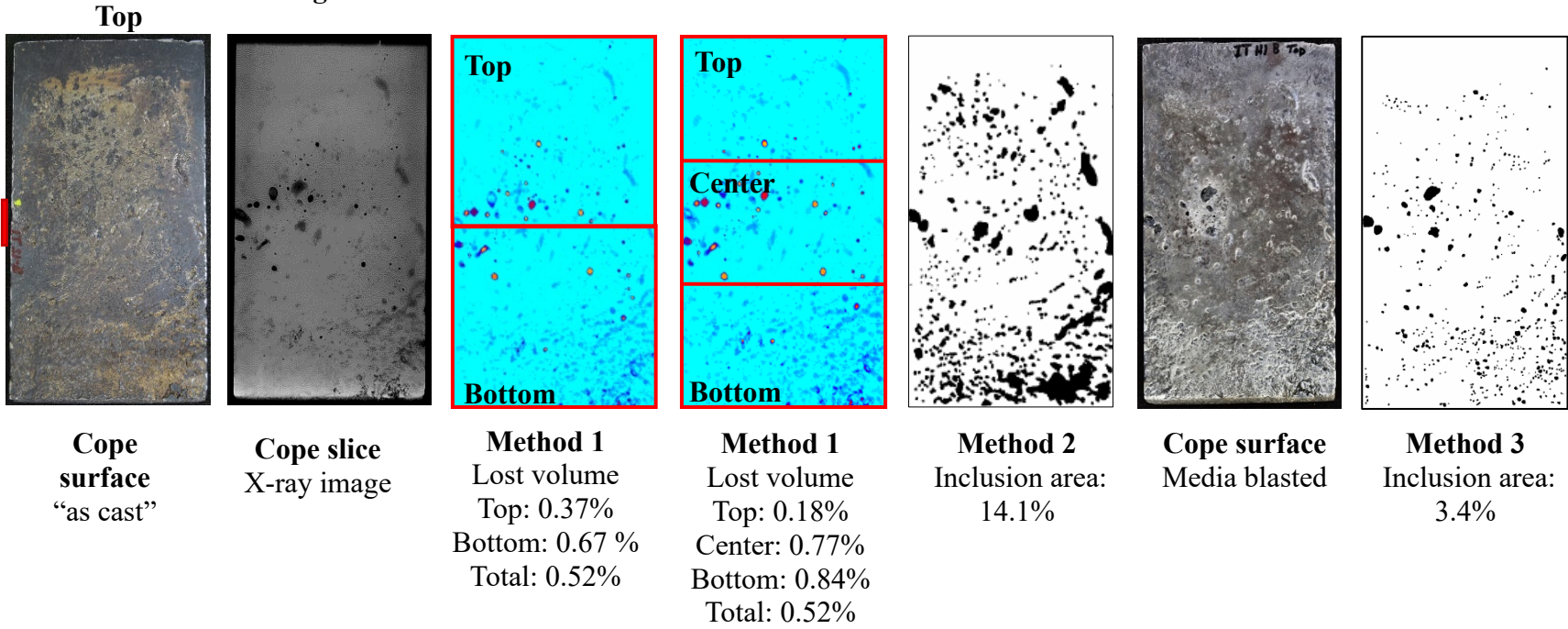
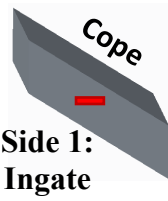
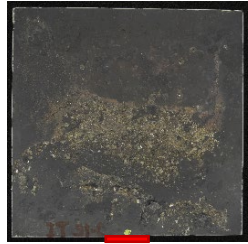
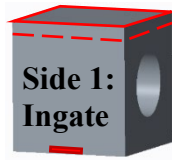
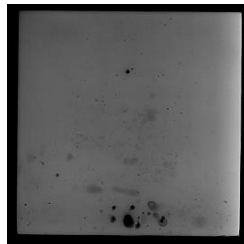


Figure 25. Images of casting surfaces and measurement results for Case 1-B using Methods 1, 2 and 3 from heat 1.

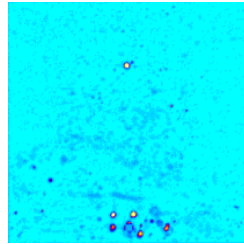
**Case 1-C
Circular Core**



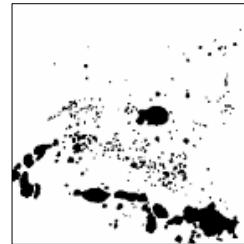
**Cope surface
"as cast"**



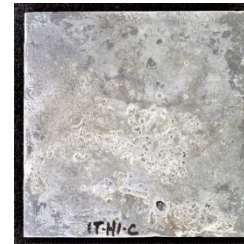
**Cope slice
X-ray image**



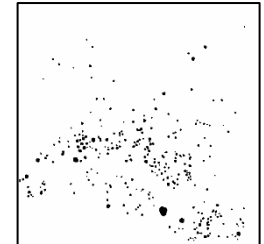
**Method 1
Lost volume: 0.44%**



**Method 2
Inclusion area: 9.1%**

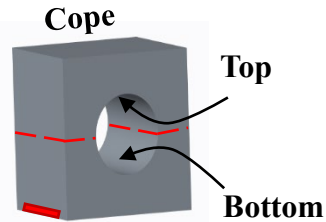


**Cope surface
Media blasted**

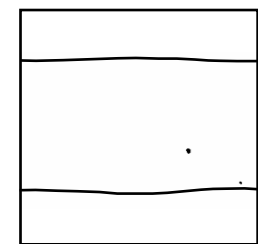
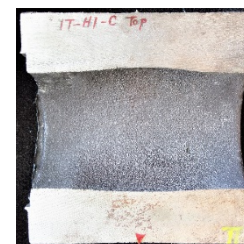
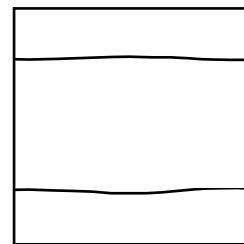


**Method 3
Inclusion area: 2.1%**

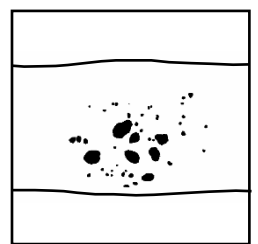
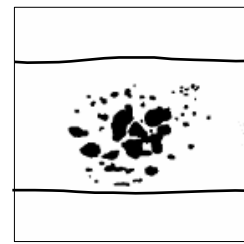
**Inside Circular
Core**



Top



Bottom



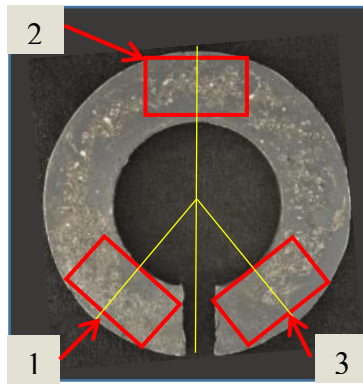
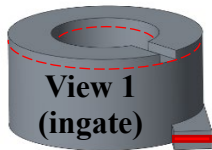
**Core surface
"as cast"**

**Method 2
Inclusion area
Top: 0%
Bottom: 7.0%**

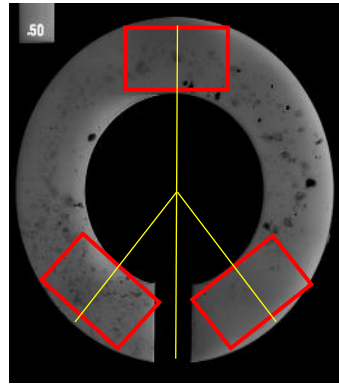
**Method 3
Inclusion area
Top: 0.1%
Bottom: 3.2%**

Figure 26. Images of casting surfaces and measurement results for Case 1-C using Methods 1, 2 and 3 from heat 1.

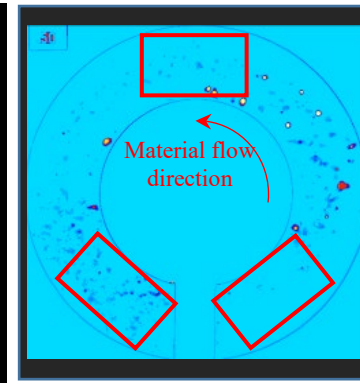
**Case 1-D
Ring with Notch
on Top**



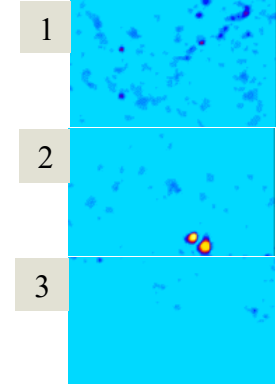
**Cope surface
"as cast"**



**Cope slice
X-ray image**



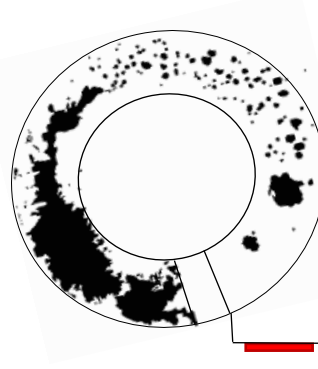
**Method 1
Lost volume: 0.98%**



Lost volume
Section 1 - 1.17%
Section 2 - 0.64%
Section 3 - 0.14%



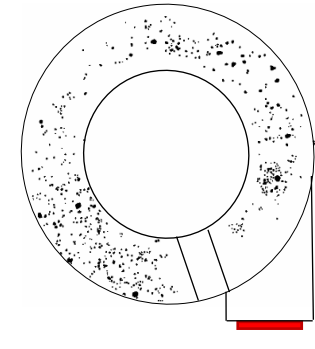
**Cope surface
"as cast"**



**Method 2
Inclusion area: 24.5%**

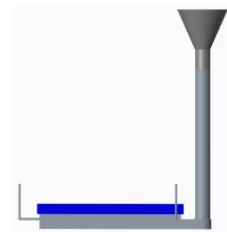
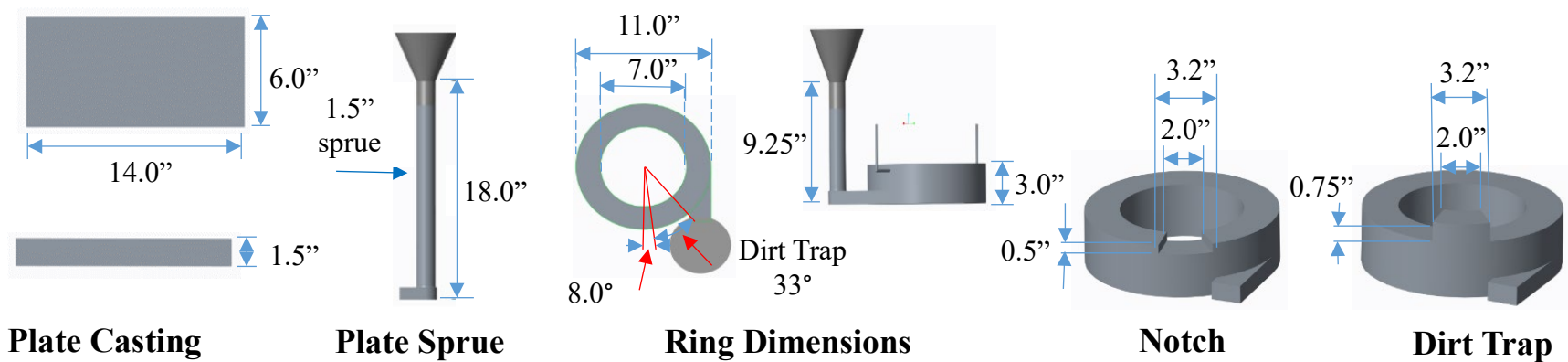


**Cope surface
Media blasted**

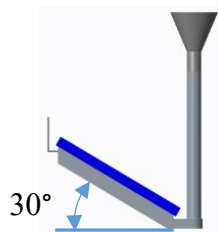


**Method 3
Inclusion area: 3.6%**

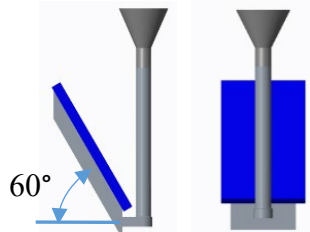
Figure 27. Images of casting surfaces and measurement results for Case 1-D using Methods 1, 2 and 3 from heat 1.



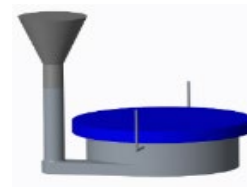
**Case 2-A
Flat**



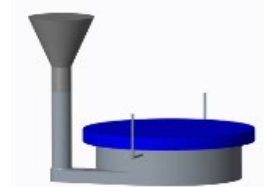
**Case 2-B
30 Degrees**



**Case 2-C
60 Degrees**



**Case 2-D
Notch on Top**



**Case 2-E
Dirt Trap on Top**

Processing information	Case 2-A	Case 2-B	Case 2-C	Case 2-D	Case 2-E
Heat number:	2	2	2	2	2
Pour order:	1/5	2/5	3/5	4/5	5/5
Pour time (s):	14.0	10.0	13.0	16.0	25.0
Pour weight (lbs):	55.2	46.9	55.2	60.7	55.6

Figure 28. Dimensional and casting process information for heat 2 inclusion tracking experiment cases.

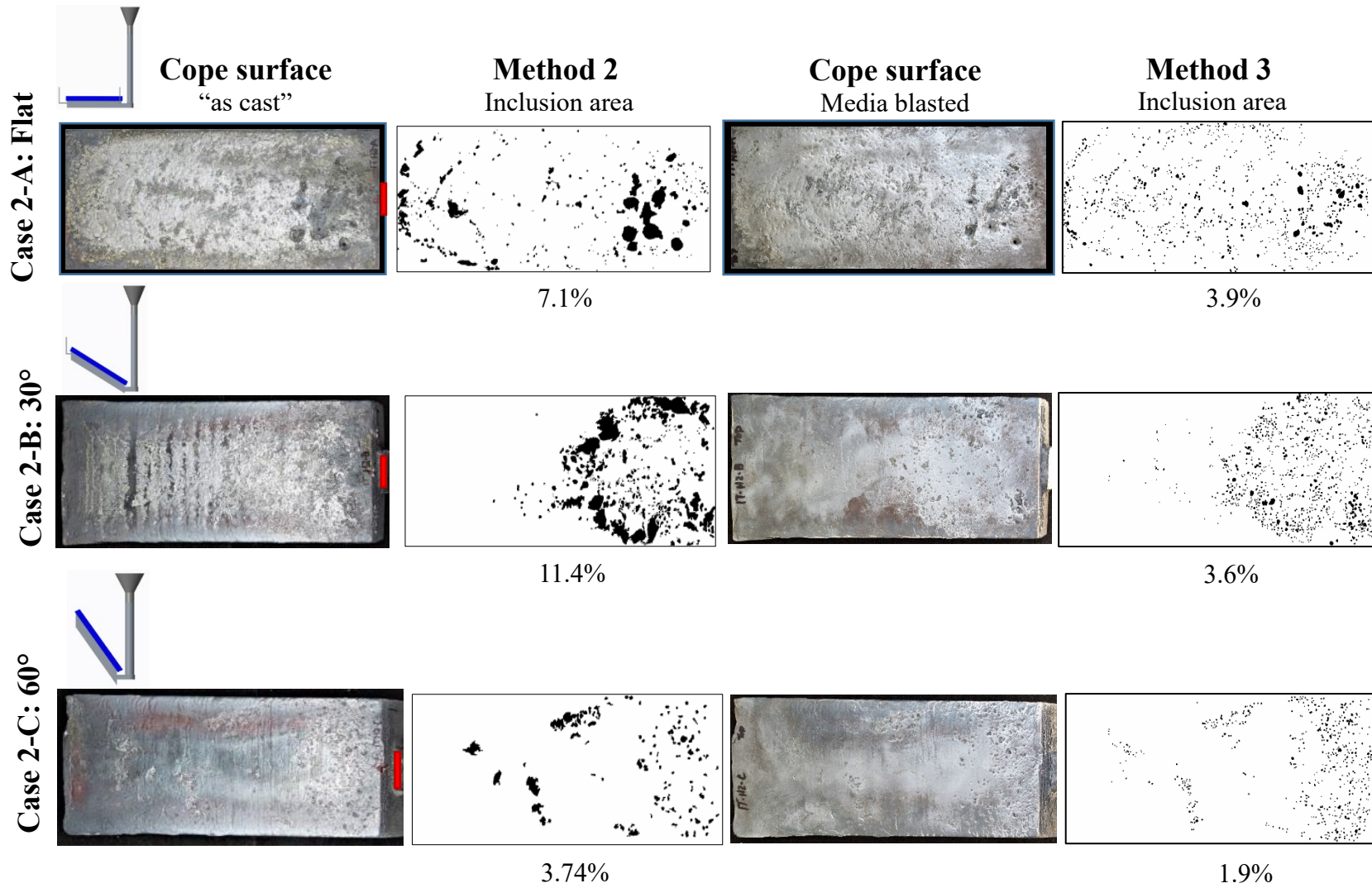


Figure 29. Images of casting surfaces and measurement results for inclined plate cases using Methods 2 and 3 from heat 2.

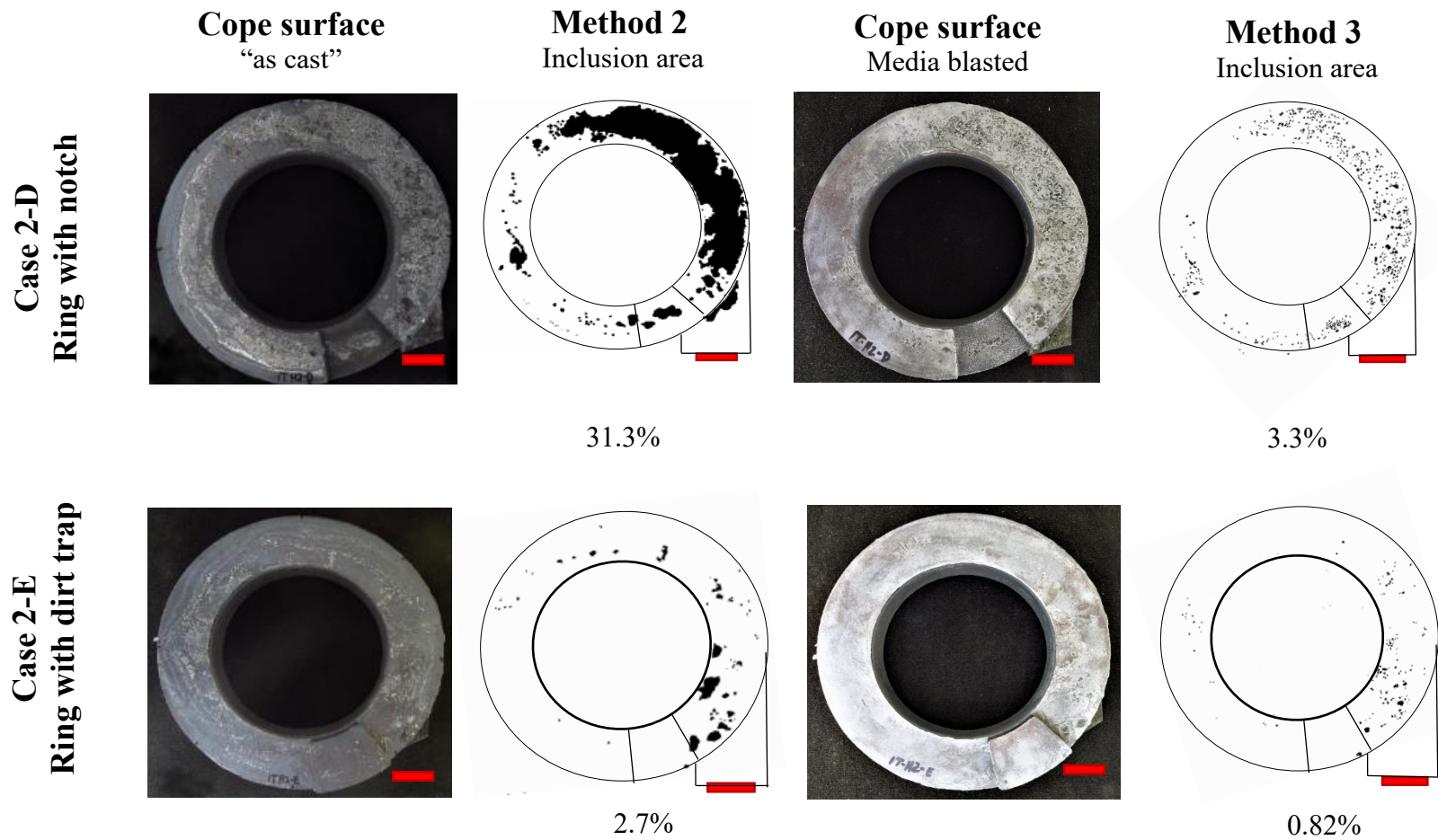


Figure 30. Images of casting surfaces and measurement results for ring casting cases using Methods 2 and 3 from heat 2.

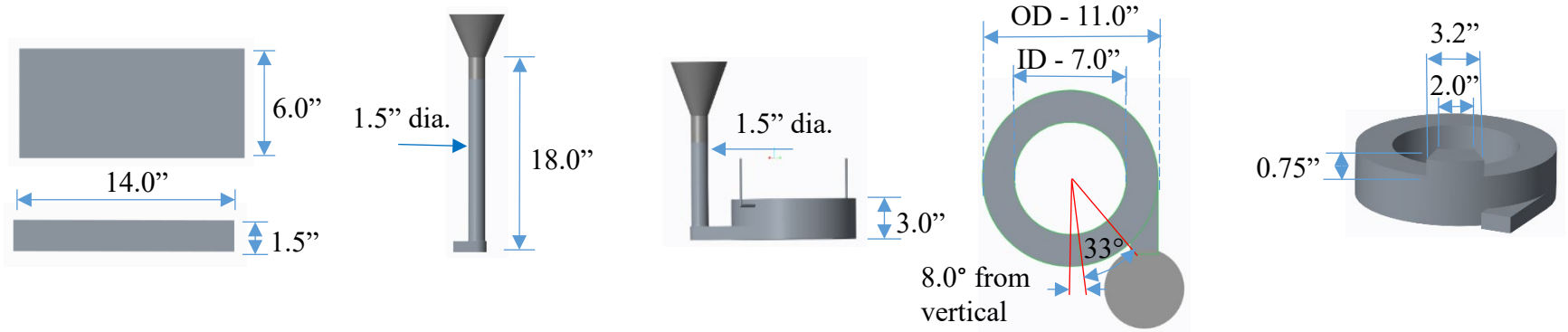
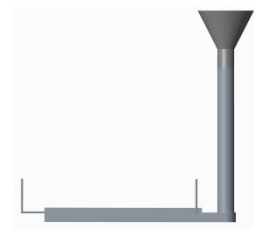


Plate Casting

Plate Sprue

Ring Dimensions

Dirt Trap Dimensions



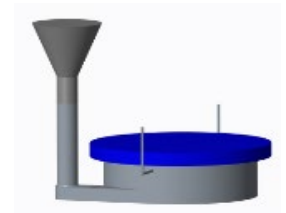
**Case 3-A
Flat Plate**



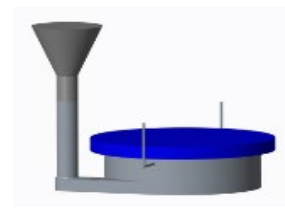
**Case 3-B
30 Degrees**



**Case 3-C
60 Degrees**



**Case 3-E
Dirt Trap on Top**



**Case 3-F
Flat Top**

Processing information

	Case 3-A	Case 3-B	Case 3-C	Case 3-E	Case 3-F
Heat number:	3	3	3	3	3 repour
Pour order:	1/4	2/4	3/4	4/4	2/2 repour
Pour time (s):	10.0	12.0	13.0	13.0	12.0
Pour weight (lbs.):	44.0	48.5	52.5	48.3	59.0

Figure 31. Dimensional and casting process information for heat 3 inclusion tracking experiment cases.

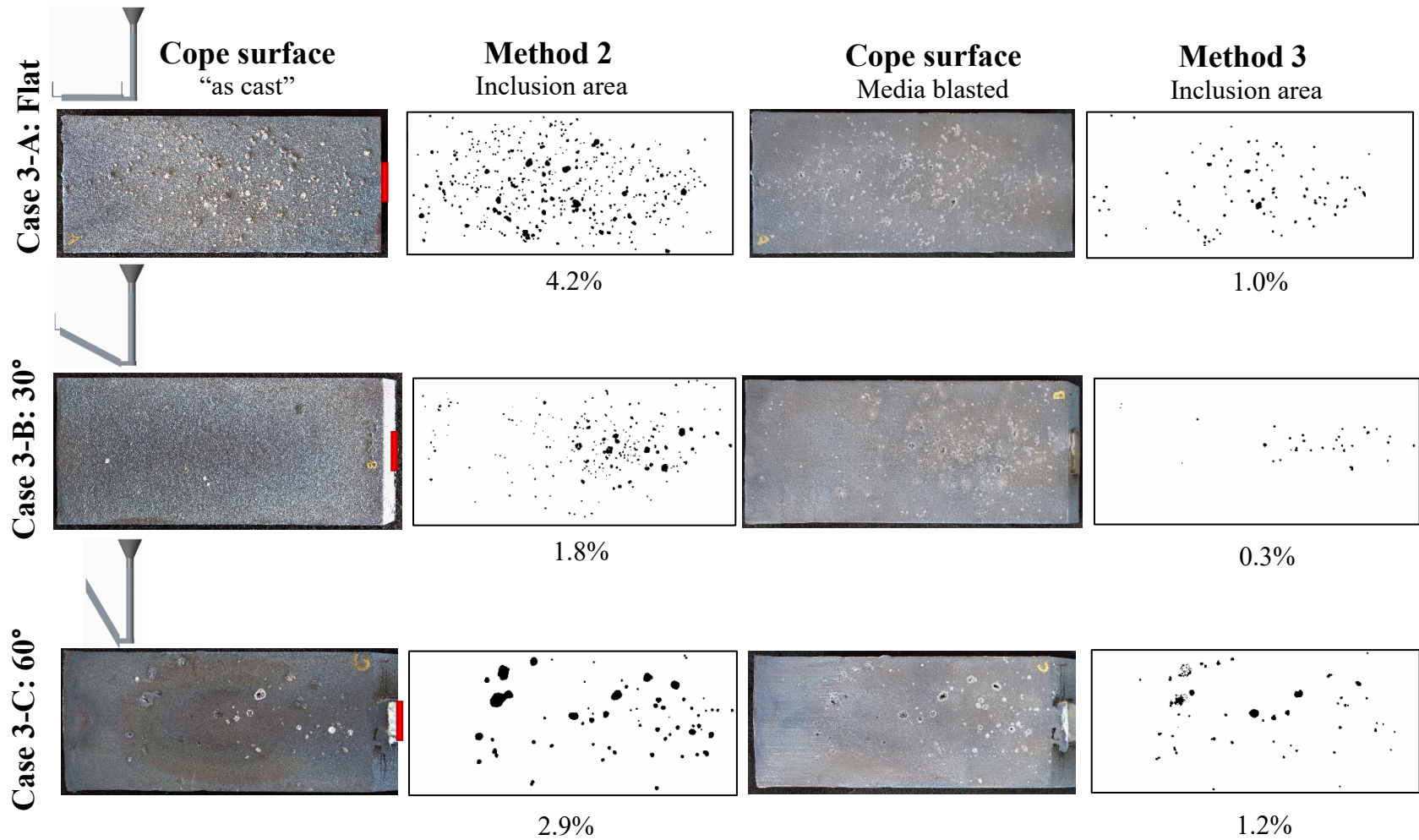


Figure 32. Images of casting surfaces and measurement results for inclined plate cases using Methods 2 and 3 from heat 3. No chill is used on the cope surface.

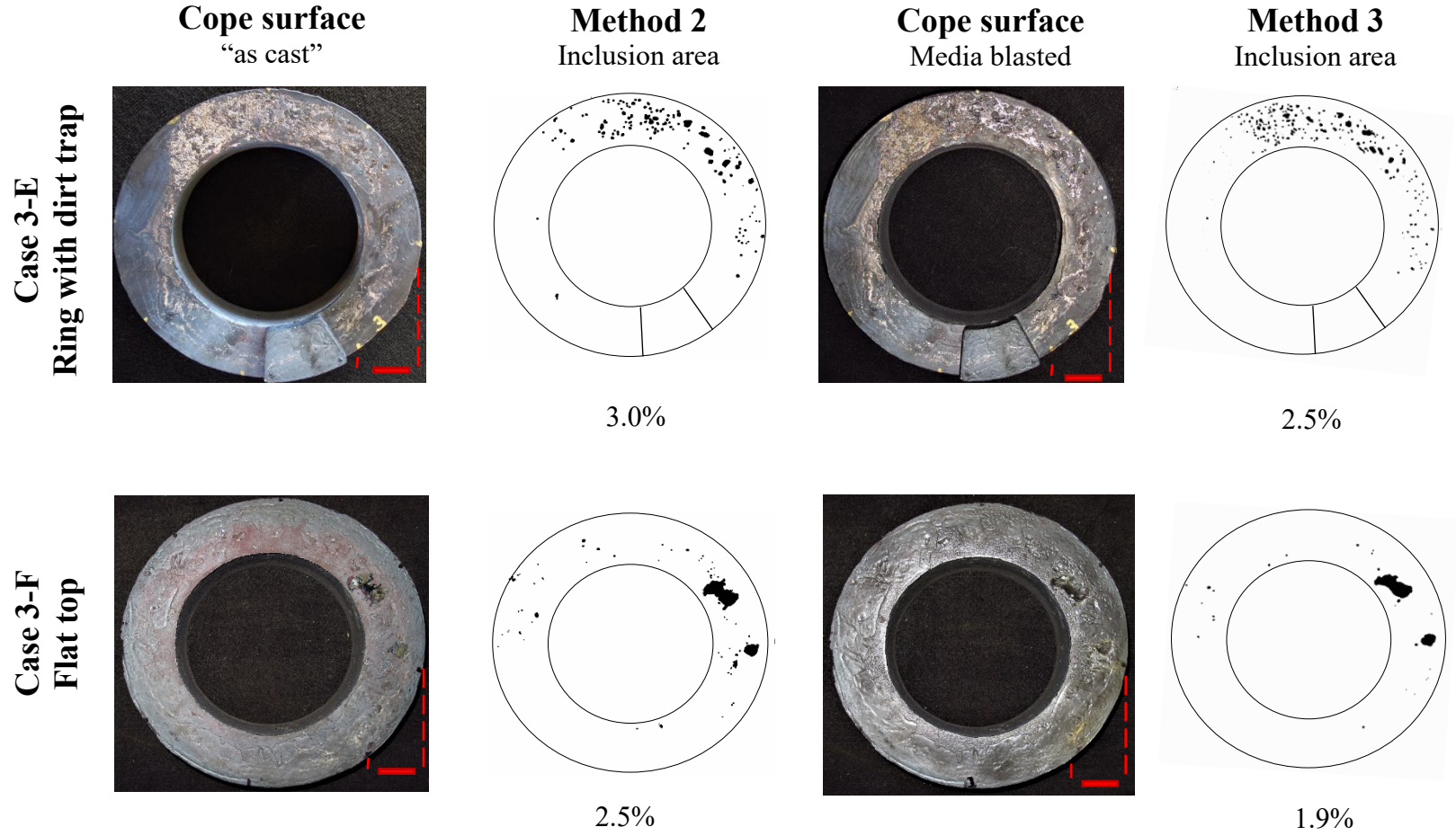


Figure 33. Images of casting surfaces and measurement results for ring casting cases using Methods 2 and 3 from heat 3.

Conclusions

Two series of casting experiments were performed investigating the generation of inclusions in the casting system, and their transport and final locations in the casting system. The first series of experiments were designed to study effect of gating system on air entrainment and inclusion generation during filling. These experiments investigated gating and sprue height effects. The second series of experiments were performed to study the effects of various casting geometries and surface orientations on the final inclusion locations and distributions within the casting experiments.

From the gating system experiments the most important finding of this work was that hardly any inclusions were generated in the gating, downsprue and runners. This was determined by locating filters in such a way to isolate the sources of the inclusions. It was found that the primary source of inclusions was from the ladle, and perhaps the pouring cup. The inclusions measured in the castings are significantly higher for all cases without using a filter. Using a filter, all castings were cleaner regardless of whether the filter is at the top of the sprue or in the runner. The results for the two filter locations were the same within the variability of the measurements, and all the gating systems produced similar results.

In the course of analyzing the gating system experiments, some conclusions about the measurements methods were made. The quantitative radiography used in Method 1 mostly measures the gas associated with the inclusions. At best it is an indirect measurement of the inclusion severity, since it is doubtful that all the gas generated is accounted for and measured. Method 2 measures more dirt and the variations within cases are larger than the differences between cases, when compared to Method 3. Method 3 involves inspecting for inclusions on a cleaned surface. Method 3 was identified as the most trustworthy, accurate and best direct inclusion measurement method used in this study.

Considering the sprue height experiments, the tallest sprue height case (27") with no metal filtering was found to consistently produce the dirtiest casting. The tallest sprue height case with filter in the runner was expected to be among the cleanest experiments. It was in only one of the two heats it was poured. In the other heat it was the third dirtiest casting out all fourteen castings poured. It was poured second in that heat, and pouring order might have been a factor in that result. The first casting poured in each heat is always dirty relative to cases poured later. The tallest sprue height case was also poured using filters at the inlet to the pouring cup and at the outlet of the cup (top of the sprue). For these cases, about half the inclusions area fraction was measured for the filter at the cup inlet case compared to the no filter case. Comparing the filter at the cup inlet case to the case with filter at the outlet of the cup, the inclusions appeared to be reduced by another factor of two for the filter at the cup outlet case. Three additional cases were poured with filters at the cup outlet (top of sprue) having sprue heights 22", 17" and 12". Two experiments were performed at each height. One of the 12" cases gave a very large inclusion measurement result by Method 2. This was probably an outlier and was a failed measurement by Method 2. Outside of that result, the 17" and 22" tall sprue cases with filter at the cup outlet were consistently the cleanest. There might be a trend in increased cleanliness for cases with filter at the cup outlet from the 27" tall sprue case to the 22" and 17" tall sprue cases, but in general there

appears no strong effect of sprue height on casting cleanliness when the filter is used at the cup outlet. All experiment cases were found to have the possibility of producing cleaner castings except for 27" tall sprue cases without filter and the 27" tall sprue with a filter at the pouring cup inlet.

To summarize conclusions from the inclusion tracking experiments, data was generated that will be used to calibrate and validate an inclusion generation and tracking model. The experimental results by themselves demonstrate the effects of various casting geometric features on the final locations of inclusions in castings. For the case with two differently inclined cope surfaces, inclusions were located at the upper ends of "peak" of the cope surfaces. Inclusions were located on the cope surface on the bottom and center portion of the casting for the inclined plate with ingate at mid-height. For the horizontal cored casting, a large amount of inclusions collected on the cope surface at the core with the inclusions clustered at the mid-length of the core. The drag side at the core was clean. On the cope surface of the cored casting, the inclusion locations were located primarily on the ingate side of the casting. For the plate castings, cope chills did not affect the locations of the inclusions. The inclusions were uniformly distributed over the cope surface for the horizontal plate castings. For plates inclined at 30 and 60 degrees, inclusions were clustered on the lower part of the cope surface to about two thirds of the way to the top of the plate. The upper third of the cope surfaces of the inclined plates were relatively clean by comparison. For the ring castings, the cope surfaces of the dirt trap cases were found to be cleaner than the notch cases. In the ring casting dirt trap experiments, the cope surfaces were clean upstream of the features, and dirt was found downstream of (after) the traps. This distribution of inclusions was found in one of the notch cases (clean upstream, dirt downstream), but in the other notch case the opposite distribution was observed (clean upstream, dirt downstream).

Even though hardly any inclusions were found to be generated in the gating systems of the gating experiments, it cannot be said that the gating system has no effect on the inclusions in a casting. The gating system still has two potential effects: (i) it filters out inclusions from the ladle (not only if a filter is used but also if the gating system has such a large cope surface that inclusions get stuck or trapped before entering the casting); (ii) as the inclusion tracking experiments show, inclusions are not evenly distributed in a casting and the location and geometry of the gating system will affect the distribution in the casting.

An area of future work was identified from the results of the gating system experiments without using filters. It was expected that the un-pressurized top ingate system would produce a much dirtier casting than the naturally pressurized, bottom filled, case using a basin. However, there was no measurable difference between them by Methods 2 and 3. The naturally pressurized case was poured first in the heat of experiments, and the un-pressurized top gated case was poured last. The first casting poured might have significantly more inclusions coming from the ladle than later castings poured. To investigate whether pouring order is an important variable in these results, additional experimental trials will be performed. Multiple castings of these un-pressurized and pressurized gating cases will be poured in three or four heats to study the effect of pouring order. By pouring a larger number of casting experiments, and using design of

experiments, a statistically meaningful dataset will be generated to understand the effect of pouring order and these two gating system on clean steel casting.

Acknowledgements

This research is sponsored by the DLA-Troop Support, Philadelphia, PA and the Defense Logistics Agency Information Operations, J68, Research & Development, Ft. Belvoir, VA. The authors also recognize Sairam Ravi and his team at the University of Northern Iowa Metal Casting Center for pouring the casting experiments.

Disclaimer

The publication of this material does not constitute approval by the government of the findings or conclusion herein. Wide distribution or announcement of this material shall not be made without specific approval by the sponsoring government activity.

References

[1] J.M. Svoboda, R.W. Monroe, C.E. Bates and J. Griffin, "Appearance and Composition of Oxide Macroinclusions in Steel Castings," AFS Transactions, Vol. 95, pp. 187-202, 1987

[2] J.A Griffin and C.E. Bates, "Ladle Treating, Pouring and Gating for the Production of Clean Steel Castings," Steel Founders' Society of America Research Report No. 104, 1991.

[3] Hardin, R.A., and Beckermann, C., "Measurement and Prediction of Mechanical Behavior of Cast Steel Plates with Centerline Porosity," in Proceedings of the 65th SFSA Technical and Operating Conference, Paper No. 5.4, Steel Founders' Society of America, Chicago, IL, 2011.

[4] Schindelin, J., Arganda-Carreras, I., and Frise, E. et al., "Fiji: An Open-Source Platform for Biological-image Analysis", Nature Methods, Vol. 9, No. 7, pp. 676-682, 2012.

[5] Melendez, A.J., Carlson, K.D., and Beckermann, C., "Modeling of Reoxidation Inclusion Formation in Steel Sand Casting," Int. J. Cast Metals Research, Vol. 23, pp. 278-288, 2010.